TRIBHUVAN UNIVERSITY
INSTITUTE OF ENGINEERING
PULCHOWK CAMPUS

Thesis no: M-63-MSMDE-2020-2023

Vibration analysis of cantilever shaft-disk system for transient response to impact jet

by

Bidhan Pandey (076MSMDE003)

A THESIS
SUBMITTED TO THE DEPARTMENT OF MECHANICAL AND AEROSPACE ENGINEERING
IN PARTIAL FULFILLMENT OF THE REQUIREMENTS FOR THE DEGREE OF MASTER OF SCIENCE IN
MECHANICAL SYSTEMS DESIGN AND ENGINEERING

DEPARTMENT OF MECHANICAL AND AEROSPACE ENGINEERING
LALITPUR, NEPAL

APRIL, 2023

COPYRIGHT

TRIBHUVAN UNIVERSITY
INSTITUTE OF ENGINEERING
PULCHOWK CAMPUS
DEPARTMENT OF MECHANICAL AND AEROSPACE ENGINEERING

The undersigned certify that they have read, and recommended to the Institute of Engineering for acceptance, a thesis entitled "Vibration Analysis of Cantilever Shaft-Disk System for Transient Response to Impact Jet" submitted by Bidhan Pandey in partial fulfillment of the requirements for the Degree of Master of Science in Mechanical Systems Design and Engineering.

_____

Supervisor, Mahesh Chandra Luintel, PhD

Professor

Department of Mechanical and Aerospace Engineering

_____

External Examiner, Er. Janak Kumar Tharu

Assistant Professor

Nepal Engineering College

_____

Committee Chairperson, Surya Prasad Adhikari, PhD

Head of Department

Department of Mechanical and Aerospace Engineering

ABSTRACT

Engineering systems such as water turbines, different types of compressors and similar rotodynamic applications are instances of shaft and disk assembly. Representation of such systems with shaft-disk assembly can be convenient to understand their dynamic response. Startup transient is considered as a critical operation in hydraulic turbines. In this work, vibration response is analyzed for transient loadings on a cantilever shaft-disk assembly to understand behavior exhibited by applications such as an overhung Pelton turbine. Mathematical model is obtained for the cantilever shaft and disk assembly. Water jet force due to impact during the starting and shutting down of a turbine unit is used as the transient excitation force. The response representing the vibration due to the impact force is derived from the governing equations of motion obtained using the mathematical model, solved and plotted using MATLAB for the first three vibration modes. The results thus obtained are validated with the results from simulation in ANSYS.

ACKNOWLEDGEMENT

I would like to convey my utmost regards to Professor Mahesh Chandra Luintel, PhD for supervising my thesis work. His utmost guidance has made completion of this work possible. I would also like to express my sincere regards to Associate Professor Surya Prasad Adhikari, PhD, Head of Department, Department of Mechanical and Aerospace Engineering and Professor Dr. Laxman Poudel, Coordinator, Master in Mechanical Systems Design and Engineering. I would also like to thank the entire family of the Department of Mechanical and Aerospace Engineering, Pulchowk Campus for the support during this thesis work.

TABLE OF CONTENTS

LIST OF TABLES

LIST OF FIGURES

LIST OF SYMBOLS

Ω	Spin speed of shaft
ρ_s	Density of shaft
A	Cross section area of shaft
E	Modulus of elasticity
F_j	Water jet force
I	Moment of inertia of shaft about transverse axes
I_d	Moment of inertia of disk about transverse axes
J	Polar moment of inertia of shaft
J_d	Polar moment of inertia of disk
M_i	Equivalent mass of the system of ith mode
C_i	Equivalent damping of the system of ith mode
K_i	Equivalent stiffness of the system of ith mode
L	Length of shaft
m_d	Mass of disk
T_s	Kinetic energy of the shaft
T_d	Kinetic energy of the disk
U_s	Potential energy of the shaft
U_d	Potential energy of the disk

LIST OF ABBREVIATIONS

ANSYS	Analysis System
MATLAB	Matrix Laboratory
ODE	Ordinary Differential Equation

CHAPTER ONE: INTRODUCTION

1.1 Background

Engineering systems such as water turbines, different types of compressors and similar rotodynamic applications are instances of shaft and disk assembly. For instance, the runner of a Pelton turbine with its bucket can be jointly taken as a single disk unit that is mounted on a simply supported or a cantilever shaft forming a shaft-disk system. Because of their high speed operation, vibration should be kept minimum from such application since the resulting cyclic stress and subsequent material fatigue can lead to failure of the structure or the components of the system. Vibration analysis in these applications is essential to avoid any undesirable deformation or structural damage. Representing the complex rotodynamic systems as a shaft-disk system and performing vibration study on such a system is a simpler approach to understand the response of the complex rotodynamic systems to any external excitation.

Any system that has inertia and elasticity can undergo vibration which is initiated when such a system is displaced from its equilibrium position due to factors like unbalance, misalignment, friction, external excitation, flow-induced vibration, earthquakes and wind. The frequency of vibration of a system after an initial disturbance with no further external excitation is the natural frequency of the system and is determined by the system's inertial and elastic properties. Likewise, amplitude of vibration is the maximum amount of displacement of a given vibrating body with respect to its nominal or equilibrium position. If this amplitude becomes high so that the resulting stress is beyond the ultimate strength of the structure of the system, then the system can fail dramatically and the purpose of vibrational study is to avoid such amplitudes. Natural frequency is a critical factor that is taken into consideration in designing these systems for avoiding such high vibration amplitudes during operation.

Vibration of a system due to its inherent property of the system in the absence of external force is called a free vibration. Initial disturbances in the form of displacement or velocity or both can initiate free vibration in a system. Vibration in a system in response to external force or motion is called a forced vibration. Likewise, vibration of a system in the absence of dissipative forces is known as an undamped vibration whereas vibration in the presence of dissipative forces is called a damped

vibration. When a system is excited by harmonic force, the system's response can be considered as a superposition of its free and forced response. The free response, under damped condition, has a negative power exponential term in its solution which causes it to decay over time whereas the forced response lasts as long as the external excitation present. On the other hand, when any system is excited by external force for a very brief interval of time i.e. by a transient input force, depending upon the duration of the force application, the effects of both the free and forced response of the system can exist for a longer duration of time than the duration of the transient force itself.

Startup transient is considered as a critical operation in hydraulic turbines. The speed of the turbines vary during startup as it goes from rest to the operating speed. Likewise, during shutdown, the speed varied from operating speed to zero. These operating conditions mark the cases of transient loading and are the subjects of study for this thesis for a cantilever shaft-disk system. The response of a shaft-disk system such as a Pelton turbine depends on the operating parameters as well as its components. Researchers have modeled rotodynamic systems as shaft-disk systems to investigate various aspects of those systems.

1.2 Problem Definition

Pelton turbines experience a large magnitude of periodic loads as a result of the interplay between the impact jet and runner buckets (Coutu et al., 2013). If the excitation coming from the jets matches the natural frequency of the hydraulic turbine, resonance occurs which is undesirable. Now, for a turbine operating at full-load condition, it operates at a near constant speed called the operating speed and is subjected to a harmonic load from the jet and exhibits a harmonic response. However, during transient stages of operation such as startup and shutdown, the turbine is subject to transient loading from the impact jet during which period the rotating speed of the turbine also varies. Being among the most critical operating conditions, response of the turbine during startup and shutdown should be studied. Such study for a cantilever shaft-disk is done here to understand the response of a more complex turbine system.

1.3 Objectives

Main Objective

- To obtain the response of a cantilever shaft-disk during transient stages of startup and shutdown with a mathematical model and to compare the results with simulation.

Specific Objectives

- To develop a mathematical model and solve for the response of the system during startup and shutdown for a cantilever shaft-disk system.
- To find numerical solutions of the system during startup and shutdown.
- To compare the responses of the mathematical model with the numerical solution during startup and shutdown.

1.4 Limitations and Assumptions

The assumptions and limitations of this work are as follows:

- The change in rotational speed of the shaft and jet force acting on the disk is assumed to be linear for the duration of startup and shutdown.
- Bearings and the disk are assumed as rigid.
- Only a single jet force is considered in the study.

CHAPTER TWO: LITERATURE REVIEW

2.1 Overview

Most devices that consume or produce power have a disk attached to a shaft. Figure 2.1 shows such a shaft-disk model for a cantilever Pelton turbine. The major components of a rotodynamic system are the shaft, the equivalent disk and bearings. During analysis, these components are assumed rigid or flexible based on their application. A given system can be modeled with different combinations of rigid or flexible assumptions for each component.

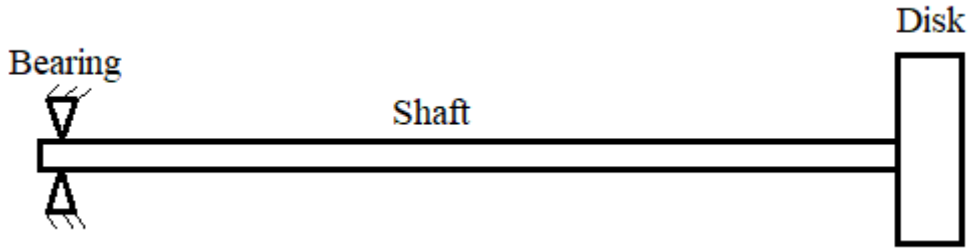

Figure 2.1 Simplified rotodynamic system for a cantilever Pelton turbine

Pelton turbine is one of the most common types of hydraulic turbines used for electricity generation in power plants. They are high head turbines and can be used for small or large power generation. These turbines are installed horizontally or vertically in the power plants and based on the position of the bearings, they can be simply supported or cantilever. They are restricted to move in the direction of the shaft axis and are free to rotate about the axis. The working principle of Pelton turbines is such that they are subject to large magnitudes of periodic loads as a result of the interplay between the impact jet and runner buckets. These loading can cause vibration in the system and can cause complete failure if the vibration amplitude goes beyond a permissible limit, which can happen when there is resonance in the system. For vibrational analysis of such a system, the shaft can be assumed as a flexible massless body in which case a discrete model can be used. On the other hand, if mass of the shaft is taken into consideration, a continuous model with infinite degrees of freedom should be used. Continuous shaft of any rotodynamic system can be modeled as a rotating Euler-Bernoulli beam as is done in this thesis.

2.2 Related Works

Khader et al. (2007) ran an experimental study to obtain the natural frequencies of a flexible shaft with multiple flexible disks. The approach of single input and single output was used to find the frequency response. Impact hammer was used to excite the system and piezoelectric accelerometer was used to record the vibration of the system. The obtained experimental response is compared with the results of an analytical approach based on assumed mode method in which free modes of vibration of the flexible disk and the flexible shaft are taken as the inputs in the assumed mode.

Zeng et al. (2012) built the differential equation for shaft vibration based on the energy of the shaft due to dynamic motion while considering both generator rotor and turbine runner. Additional forces like bearing reactions, sealing force and so on are used as inputs to the system.

Rajak et al. (2014) developed a mathematical model to obtain kinetic and potential energy of a simply supported Pelton turbine assembly. Dynamic analysis of the system was done using the energy method to obtain the natural frequency. Validation is done using modal analysis.

Motra & Luintel (2017) modeled a Pelton turbine unit with a centrally located runner with rigid property and supported simply on rigid bearings. Governing equations were obtained using the Lagrange equation which were solved with the Rayleigh-Ritz method analytically. Natural frequency obtained for discrete systems with effective masses is compared with a continuous model.

Karki et al. (2017) presented the modeling of excitation from a water jet by using the method of Fourier series. Kinetic as well as the potential energies of shaft and disk were calculated and a mathematical model was developed for the system. Equations of motion for forced vibration condition were derived with the methods of Lagrange's equation, virtual work and Rayleigh-Ritz method. The methodologies developed were used to obtain analytical solutions of the response exhibited by the pelton turbine under study.

Luintel M. (2019) presented the methodology for finding the response exhibited by the Pelton turbine shaft. Critical speeds of the unit were determined from the free vibration analysis. Likewise steady state vibration amplitudes were obtained for forced vibration due to an impact jet. Mathematical models were obtained for transverse vibration with the flexible shaft and rigid disk assumption. Shaft was modeled both as a rotating Euler-Bernoulli beam and Timoshenko beam and equations of motion were obtained for both. Critical frequencies and response due to impact jet were determined for both the models and the results were compared with those from experimental study.

Egusquiza et al. (2019) carried out an experimental study on an existing Pelton turbine unit. Modal response of the runner was studied for following cases: suspended runner, runner attached to the shaft and with the machine in operation. Sensors like acoustic emission sensor and accelerometer were used for the study. Vibration responses were recorded for transient stages with different loads on the machine. Finite Element Method based numerical model was developed to better understand the response of these turbines. Finally, frequencies sensed during machine operation were compared with those from the numerical model and the effect of various factors on response of the runner was analyzed.

Bhandari et al. (2019) carried out research to model the forced excitation of impact jet force as a Fourier series and to obtain corresponding reaction for a cantilever Pelton turbine by developing a mathematical model. The forced vibration amplitude thus calculated was verified with the results from simulation in ANSYS. The effect of change in rotational speed on the vibration amplitude of the shaft was also studied. Natural modes of vibration and equations of motion were derived with the use of the Rayleigh-Ritz method followed by Lagrange's equation. Vibration amplitudes in the jet direction and in other transverse directions due to a single impact jet were obtained for the turbine unit and the results were compared with the results obtained from simulation.

Luintel & Bajracharya (2019) presented a method for studying the dynamic response exhibited by Pelton turbine shaft in response to water jet force. Lagrange equation of motion in combination with assumed mode method was used to obtain bending

vibration of the turbine assembly in transverse directions. The runner was assumed as a rigid body while the shaft was assumed as Euler-Bernoulli. Fourier series is used to model the force due to impact from the water jet. Free vibration analysis of the turbine system was done to obtain critical speeds of the system which is presented in the form of Campbell diagram and forced response analysis was done to obtain the reaction of the turbine system to the impact jet; both analysis was done considering the first three modes of vibration only.

Jirel et al. (2021) researched on modeling the excitation force of the impact of water jet as a Fourier series to obtain the dynamic reaction of an overhung Pelton turbine unit by mathematical model development. Vibration amplitude obtained analytically was compared with the simulated results from ANSYS. Mathematical model was obtained by evaluating the total energy, kinetic and potential, of the shaft-disk system including that of the unbalanced mass. Equations of motion representing the unbalanced shaft-disk system were obtained by applying Lagrange's equation. The results that were obtained were validated from the simulation in ANSYS. Runner was modeled as a disk attached to the free end of a flexible shaft having fixed support boundary condition at the other end.

Egusquiza et al. (2021) have analyzed the transient phase of start-up of Pelton turbines. Experimental study was done on a horizontal shaft Pelton turbine prototype. Natural frequencies and the corresponding mode shapes were acquired from impact testing with the help of multiple accelerometers on the runner, shaft and the bearings. It was observed that the initial impact of the jet on the stationary turbine caused larger amplitudes of vibration. Also, after the turbine started to rotate, vibration levels increased each time the frequency of excitation matched the natural frequency.

2.3 Research Gap

The researches so far have mostly focused on the steady-state response for a turbine system with flexible shaft. In the last study mentioned above, a startup transient response was found using an experimental approach. In this thesis, a mathematical model will be developed for a shaft-disk system for a cantilever type shaft-disk assembly and the response of the system for startup and shutdown conditions will be acquired.

CHAPTER THREE: METHODOLOGY

3.1 Thesis framework

Figure 3.1 shows the overall framework of the thesis. Mathematical Model is developed for the cantilever shaft-disk system and solved using MATLAB. The results are compared with those from ANSYS simulation.

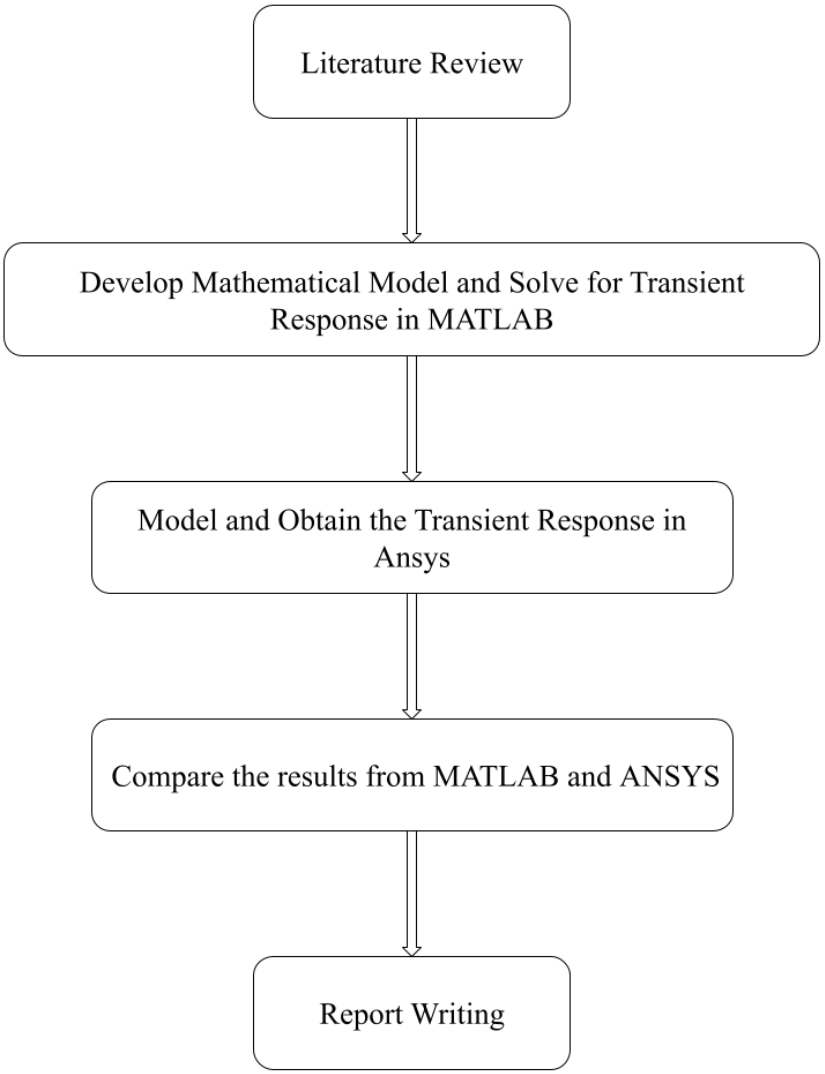

Figure 3.1 Framework of the Thesis

3.2 Literature review

Works done in the field of vibrational analysis of rotodynamic systems as shaft-disk systems are collected. These studies are used to develop a suitable mathematical model for the system.

3.3 Mathematical model development

Energy method is selected as the suitable technique for developing the mathematical model from the literature. The kinetic and potential energies for the shaft-disk system are calculated and Lagrange's equations and method of assumed modes is used to obtain the governing equations of motion. For this thesis, the disk and the bearings are taken as rigid and only the shaft is assumed to be flexible.

3.4 Research tools

Following tools will be used for the completion of the project:

- MATLAB
- ANSYS Mechanical

3.5 Response of the system using MATLAB

Data for a simply supported Pelton turbine is taken from the model present at the Department of Mechanical and Aerospace Engineering, Pulchowk Campus, given in Appendix A. The length of cantilever Pelton turbine for this thesis is obtained by finding the equivalent length for the same deflection at the end of the cantilever shaft as that for this simply supported Pelton turbine. Governing equations are solved using a MATLAB program for startup and shutdown as provided in Appendix B. Deformation of the shaft with respect to time is plotted as the response of the system to external excitation.

3.6 Modeling and Analysis in ANSYS

Simulation of the problem is done using ANSYS 2022. The system to be analyzed will be defined in the relevant module of the software. The software solves the problem by discretizing the model into finite elements and obtaining the equivalent system of algebraic equations for the problem. For this thesis work, initially modal analysis will be done followed by transient structural analysis.

3.6.1 Modal Analysis

The modules for modal analysis in ANSYS is discussed below:

1. Engineering Data

The Engineering Data section of ANSYS is a database of common engineering materials with their mechanical properties. For this work, shaft material is added to the database of Engineering Data defining its isotropic stiffness and density.

2. Geometry

Shaft is defined as a line body with circular cross-section defined for it. The disk is assumed to be rigid and is modeled as a point mass with mass and mass moment of inertia defined later in the Model part of the analysis. The point mass is attached to the free end of the line body of the shaft.

3. Model

Bearing connection is provided at one end of the shaft in this part. In order to model the bearing as a rigid body, very high stiffness is defined. Meshing is done to discretize the continuous line body of the shaft into smaller elements. Element size and order is also defined.

4. Setup

One remote displacement at the bearing end of the shaft is provided for free rotation about the longitudinal axis of the shaft while restricting axial motion along the same axis..

5. Solutions

The solver converts governing equations into algebraic equations and computes field variables. A solver computes the unknown field variables.

6. Results

Natural frequencies of the system are obtained in this section and the corresponding mode shape or the response is used for transient structural analysis.

3.6.2 Transient Structural Analysis

1. Setup

The force and rotational velocity inputs to the system are defined in this section. Rotational velocity and impact force are assumed to vary linearly during the excitation period of startup and shutdown. Time step controls are defined here.

2. Solutions

The governing equations are converted into algebraic equations and solved to obtain the displacement of nodes.

3. Results

Total deformation of the shaft in the direction of the jet is obtained in the Results.

3.7 Documentation

Documentation is done for the entire duration of the thesis work from literature review to final report. There are six chapters in the final report from Introduction to Conclusions and Recommendations. Introduction, the first chapter, includes background, problem definition, objectives and limitations of the thesis. In the second chapter, literature review is included and the research gap is discussed. Third chapter outlines and discusses the methodology of this work. Chapter four includes the mathematical model development and simulation setup. Chapter five is on the results from the mathematical model and simulation. Lastly, Chapter six is the conclusions and recommendations of this work.

CHAPTER FOUR: MATHEMATICAL MODEL DEVELOPMENT

4.1 Kinematics of the shaft-disk system

FIgure 4.1 shows a cantilever shaft-disk system with its coordinate axes defined. The length of the shaft is L, axis X is along the longitudinal axis of the shaft, axis Y is defined perpendicular to the plane of the paper and axis Z is defined in the vertical direction. The deflection in the horizontal plane in the direction of Y axis is defined as v(x,t) and the deflection in the vertical plane in the direction of Z axis is defined as w(x,t) Water jet impacts the disk in the Y direction.

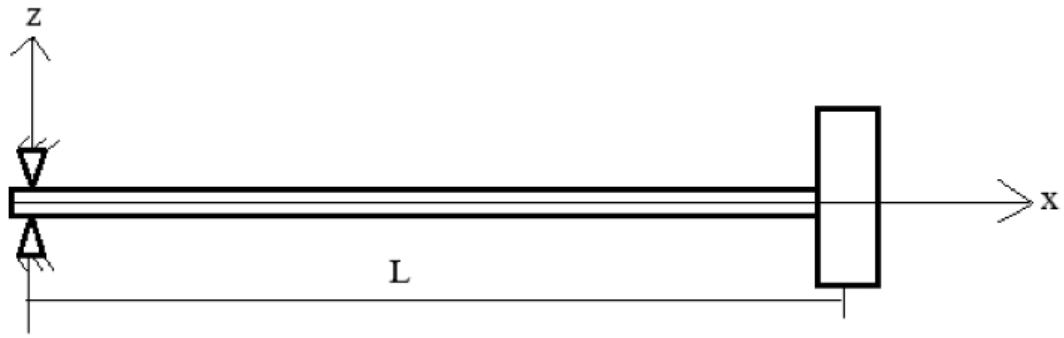

Figure 4.1 Shaft-disk system

Kinematics of Shaft

Let the angular velocity of the shaft be Ω. In vector form,

$$\omega_s = \Omega \vec{i} \qquad \text{Eq.4.1}$$

Neutral axis position vector is

$$r_s = v\vec{j} + w\vec{k} \qquad \text{Eq.4.2}$$

Velocity vector of typical point on neutral axis of the shaft is

$$v_s = \dot{r}_s^{\rightarrow} + \omega_s^{\rightarrow} * r_s^{\rightarrow} \qquad \text{Eq.4.3}$$

$$v_s = (\dot{v} - \Omega w)\vec{j} + (\dot{w} + \Omega v)\vec{k} \qquad \text{Eq.4.4}$$

Kinematics of the Disk

Angular velocity vector of the shaft element is

$$\omega_d = [(\Omega + v'\dot{w}')\vec{i} + (-\Omega v' - \dot{w}')\vec{j} + (-\Omega w' + \dot{v}')\vec{k}] \qquad \text{Eq.4.5}$$

(Khanlo et al., 2011)

4.2 Energy Method

4.2.1 Energy of the components

The shaft is assumed to be a flexible member and thus poses potential energy as well in addition to the kinetic energy which are given below.

Kinetic Energy of Rotating Shaft

$$T_s = \frac{1}{2}\rho_s A \int_0^L [(\dot{v} - \Omega w)^2 + (\dot{w} + \Omega v)^2]\, dx + \frac{1}{2}\rho_s J_s \int_0^L [(\Omega + v'\dot{w}')^2]\, dx$$
$$+ \frac{1}{2}\rho_s I_s \int_0^L [(-\Omega v' - \dot{w}')^2 + (-\Omega w' + \dot{v}')^2]\, dx \qquad \text{Eq.4.6}$$

Where,

Ω = Rotational speed of shaft

ρs = Density of shaft

A = Shaft cross section area

Js = Polar moment of inertia of shaft

Is = Area moment of inertia of shaft about transverse axes

v and w = translational velocity about Y and Z axis respectively

Potential Energy of Rotating Shaft

The potential energy in the shaft due to bending is given by:

$$U_s = \frac{1}{2} E I_s \int_0^L [(v'')^2 + (w'')^2] dx \qquad \text{Eq.4.7}$$

Where,

E = Shaft modulus of elasticity

Is = Area moment of inertia of shaft about transverse axes

For simplicity of the analysis, the disk is assumed as a rigid body and thus its potential energy is zero. The total kinetic energy of the disk is the sum of its translational and rotational kinetic energies.

Kinetic Energy of Disk

$$T_d = \left[\frac{1}{2}[m_d\,[(\dot{v} - (\Omega w)^2 + (\dot{w} + \Omega v)^2] + \frac{1}{2}\rho_d h\, J_d(\Omega + v'\dot{w}')^2\right.$$
$$\left. + \frac{1}{2}\rho_d h\; I_d(-\Omega v' - \dot{w}')^2 + \frac{1}{2}\rho_d h\, I_d(-\Omega w' + \dot{v}')^2)\right]\Big|_{x=L} \qquad \text{Eq.4.8}$$

Where,

md = Mass of disk

ρd = Density of disk

Js = Area polar moment of inertia of disk about x-x axis Is = Area moment of inertia of disk about y-y or z-z axis

h = Thickness of runner

Potential Energy of Disk

The potential energy of the disk is zero since it is assumed as a rigid body.

$U_d = 0$ Eq.4.9

4.2.2 Excitation force

The source of external excitation for a pelton turbine is the impact jet that hits the bucket of the pelton turbine. During startup, the speed of the turbine goes from zero to a constant value equal to the operating speed. During this interval the excitation force is assumed to go from zero to a constant value. Likewise, during shutdown, the external excitation is assumed to go from a constant value to zero.

Karki et al. (2017) has evaluated the jet force for the pelton turbine system given in Appendix A as:

$F_j = 193$ N

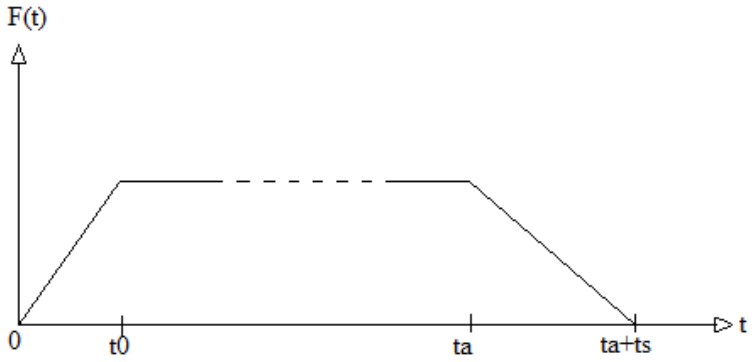

Figure 4.2 Startup and shutdown excitation for a pelton turbine

Change in transient input for startup and shutdown both are assumed to be linear as shown in Figure 4.2.

Function of startup excitation force:

$F = (F_j/t_0)\, t\, (1-u(t-t_0)) + F_j\, u(t-t_0)$ Eq.4.11

The start-up transient period is the period between the opening of the nozzle and the turbine reaching nominal speed i.e., t_0.

Let's assume, start-up transient period is $t_0 = 5$ s

Function of shutdown excitation force:

$F = [F_j - (F_j / t_s)(t - t_a)] [u(t - t_a) - u(t - (t_a + t_s)]$ Eq.4.12

Let us consider shutdown begins at t_a = 300 s and completed at t_b = 310 s with shutdown period of t_s = 10 s.

Work done by the impact of the jet is:

$W_{ext} = F(t)v|_{x=L}$ Eq.4.13

4.2.3 Equivalent length for cantilever pelton turbine

Data in Appendix A is for the simply supported pelton turbine. The length of the shaft for the cantilever pelton turbine is obtained by equating deflections in the turbines while at rest if the same force is applied on both of them.

For simply supported beam,

If force F is applied at the center of the beam, deflection at the center of the beam is:

$D_1 = FL'^3/48EI$

Where L': Length of the simply supported beam

For a cantilever beam,

If force F is applied at the end of the beam, deflection at the end of the beam is:

$D_2 = FL^3/3EI$

Where L: Length of the cantilever beam

(Beer et al., 2011)

Now,

Equating D_1 and D_2,

$FL'^3/48EI = FL^3/3EI$

i.e. L = 0.1875 L'

From Appendix A, L' = 519 mm

Then, L = 97.3125 mm

4.2.4 Assumed Mode Method

Using assumed mode method, the displacement variable is

$v = \{\phi(x)^T \{V(t)\} = \{\phi\}^T \{V\}$ Eq.4.14

$w = \{\phi(x)\}^T \{W(t)\} = \{\phi\}^T \{W\}$ Eq.4.15

Where,

$\phi(x)$ is the spatial function describing the transverse deflection

V(t) and W(t) are vectors corresponding to the time dependent coordinates.

4.2.5 Total Energy of the System

Total Kinetic Energy

Expanding Eq.4.6, neglecting small terms and using Eq.4.14 and 4.15, we get,

Kinetic energy of the shaft:

$$T_s = \frac{1}{2}\rho_s A\int_0^L \{\dot{V}\}\{\phi\}^T\{\phi\}\{\dot{V}\}^T dx - \rho_s A\Omega\int_0^L \{\dot{V}\}\{\phi\}^T\{\phi\}\{W\}^T dx$$
$$+ \frac{1}{2}\rho_s A\Omega^2\int_0^L \{W\}\{\phi\}^T\{\phi\}\{W\}^T dx + \frac{1}{2}\rho_s A\int_0^L \{\dot{W}\}\{\phi\}^T\{\phi\}\{\dot{W}\}^T dx$$
$$+ \rho_s A\Omega\int_0^L \{\dot{W}\}\{\phi\}^T\{\phi\}\{V\}^T dx + \frac{1}{2}\rho_s A\Omega^2\int_0^L \{V\}\{\phi\}^T\{\phi\}\{V\}^T dx$$
$$+ \frac{1}{2}\rho_s J_s\Omega^2 L + \rho_s J_s\Omega\int_0^L \{V\}\{\phi'\}^T\{\phi'\}\{\dot{W}\}^T dx + \frac{1}{2}\rho_s I_s\Omega^2\int_0^L \{V\}\{\phi'\}^T\{\phi$$
$$'\}\{V\}^T dx + \rho_s I_s\Omega\int_0^L \{V\}\{\phi'\}^T\{\phi'\}\{\dot{W}\}^T dx + \frac{1}{2}\rho_s I_s\int_0^L \{\dot{W}\}\{\phi'\}^T\{\phi'\}\{\dot{W}\}^T$$
$$dx + \frac{1}{2}\rho_s I_s\Omega^2\int_0^L \{W\}\{\phi'\}^T\{\phi'\}\{W\}^T dx - \rho_s I_s\Omega\int_0^L \{W\}\{\phi'\}^T\{\phi'\}\{\dot{V}\}^T dx$$
$$+ \frac{1}{2}\rho_s I_s\int_0^L \{\dot{V}\}\{\phi'\}^T\{\phi'\}\{\dot{V}\}^T dx$$

Eq.4.16

Likewise, expanding Eq.4.8, neglecting small terms and using Eq.4.14 and 4.15, we get,

Kinetic energy of the disk:

$$
\begin{aligned}
T_d = {} & \frac{1}{2} m_d \{\dot{V}\} \{\phi\}_d^T \{\phi\}_d \{\dot{V}\}^T - m_d \Omega \{\dot{V}\} \\
& \{\phi\}_d^T \{\phi\}_d \{W\}^T + \frac{1}{2} m_d \Omega^2 \{W\} \\
& \{\phi\}_d^T \{\phi\}_d \{W\}^T + \frac{1}{2} m_d \{\dot{W}\} \{\phi\}_d^T \{\phi\}_d \\
& \{\dot{W}\}^T + m_d \Omega \{\dot{W}\} \{\phi\}_d^T \{\phi\}_d \{V\}^T \\
& + \frac{1}{2} m_d \Omega^2 \{V\} \{\phi\}_d^T \{\phi\}_d \{V\}^T \\
& + \frac{1}{2} \rho_d h J_d \Omega^2 + \rho_d h J_d \Omega \{V\} \{\phi'\}_d^T \{\phi'\}_d \\
& \{\dot{W}\}^T + \frac{1}{2} \rho_d h J_d \Omega^2 \{V\} \{\phi'\}_d^T \{\phi'\}_d \{V\}^T \\
& + \rho_d h I_d \Omega \{V\} \{\phi'\}_d^T \{\phi'\}_d \{\dot{W}\}^T \\
& + \frac{1}{2} \rho_d h I_d \{\dot{W}\} \{\phi'\}_d^T \{\phi'\}_d \{\dot{W}\}^T \\
& + \frac{1}{2} \rho_d h I_d \Omega^2 \{W\} \{\phi'\}_d^T \{\phi'\}_d \{W\}^T \\
& - \rho_d h I_d \Omega \{W\} \{\phi'\}_d^T \{\phi'\}_d \{\dot{V}\}^T \\
& + \frac{1}{2} \rho_d h I_d \{\dot{V}\} \{\phi'\}_d^T \{\phi'\} \{\dot{V}\}^T
\end{aligned}
\qquad \text{Eq.4.17}
$$

Total kinetic energy of the system is:

$T = T_s + T_d$

$$T = \frac{1}{2}\rho_s A\int_0^L \{\dot{V}\}\{\phi\}^T\{\phi\}\{\dot{V}\}^T dx - \rho_s A\Omega\int_0^L \{\dot{V}\}\{\phi\}^T\{\phi\}\{W\}^T dx + \frac{1}{2}\rho_s A\Omega^2$$
$$\int_0^L \{W\}\{\phi\}^T\{\phi\}\{W\}^T dx + \frac{1}{2}\rho_s A\int_0^L \{\dot{W}\}\{\phi\}^T\{\phi\}\{\dot{W}\}^T dx + \rho_s A\Omega\int_0^L \{\dot{W}\}\{\phi\}^T\{\phi\}\{V\}^T dx$$
$$+ \frac{1}{2}\rho_s A\Omega^2\int_0^L \{V\}\{\phi\}^T\{\phi\}\{V\}^T dx + \frac{1}{2}\rho_s J_s\Omega^2 L + \rho_s J_s\Omega\int_0^L \{V\}\{\phi'\}^T\{\phi'\}\{\dot{W}\}^T dx$$
$$+ \frac{1}{2}\rho_s I_s\Omega^2\int_0^L \{V\}\{\phi'\}^T\{\phi'\}\{V\}^T dx + \rho_s I_s\Omega\int_0^L \{V\}\{\phi'\}^T\{\phi'\}\{\dot{W}\}^T dx + \frac{1}{2}\rho_s I_s\int_0^L \{$$
$$\dot{W}\}\{\phi'\}^T\{\phi'\}\{\dot{W}\}^T dx + \frac{1}{2}\rho_s I_s\Omega^2\int_0^L \{W\}\{\phi'\}^T\{\phi'\}\{W\}^T dx - \rho_s I_s\Omega\int_0^L \{W\}\{\phi'\}^T\{\phi'\}\{\dot{V}\}^T$$
$$dx + \frac{1}{2}\rho_s I_s\int_0^L \{\dot{V}\}\{\phi'\}^T\{\phi'\}\{\dot{V}\}^T dx + \Big[\frac{1}{2}m_d\{\dot{V}\}\{\phi\}_d^T\{\phi\}_d\{\dot{V}\}^T - m_d\Omega\{\dot{V}\}\{\phi\}_d^T\{\phi\}_d$$
$$\{W\}^T + \frac{1}{2}m_d\Omega^2\{W\}\{\phi\}_d^T\{\phi\}_d\{W\}^T + \frac{1}{2}m_d\{\dot{W}\}\{\phi\}_d^T\{\phi\}_d\{\dot{W}\}^T + m_d\Omega\{\dot{W}\}\{\phi\}_d^T\{\phi\}_d$$
$$\{V\}^T + \frac{1}{2}m_d\Omega^2\{V\}\{\phi\}_d^T\{\phi\}_d\{V\}^T + \frac{1}{2}\rho_d hJ_d\Omega^2 + \rho_d hJ_d\Omega\{V\}\{\phi'\}_d^T\{\phi'\}_d\{\dot{W}\}^T$$
$$+ \frac{1}{2}\rho_d hJ_d\Omega^2\{V\}\{\phi'\}_d^T\{\phi'\}_d\{V\}^T + \rho_d hI_d\Omega\{V\}\{\phi'\}_d^T\{\phi'\}_d\{\dot{W}\}^T + \frac{1}{2}\rho_d hI_d\{\dot{W}\}$$
$$\{\phi'\}_d^T\{\phi'\}_d\{\dot{W}\}^T + \frac{1}{2}\rho_d hI_d\Omega^2\{W\}\{\phi'\}_d^T\{\phi'\}_d\{W\}^T - \rho_d hI_d\Omega\{W\}\{\phi'\}_d^T\{\phi'\}_d\{\dot{V}\}^T$$
$$+ \frac{1}{2}\rho_d hI_d\{\dot{V}\}\{\phi'\}_d^T\{\phi'\}\{\dot{V}\}^T\Big]$$

Eq.4.18

Total Potential Energy of the System

Total potential energy of the system is sum of potential energy of shaft and disk or rotor which is given by: $U = U_s + U_d$

From Eq.4.7, 4.9, 4.14 and 4.15,

$$U = \frac{1}{2}EI_s\int_0^L \{V\}^T\{\phi''\}\{\phi''\}^T\{V\}dx + \frac{1}{2}EI_s\int_0^L \{W\}^T\{\phi''\}\{\phi''\}^T\{W\}dx \quad \text{Eq.4.19}$$

Again, from Eq.4.13 and 4.14,

$$W_{ext} = F(t)\{V\}^T\{\phi\}|_{x=L} \quad \text{Eq.4.20}$$

4.2.6 Lagrangian Equation of Motion

The equations of motion for the given system can be obtained using Lagrange's equation:

$$\frac{d}{dt}\left(\frac{\partial T}{\partial \dot{q}}\right) - \left(\frac{\partial T}{\partial q}\right) + \left(\frac{\partial U}{\partial q}\right) - \left(\frac{\partial W_{ext}}{\partial q}\right) = 0 \quad \text{Eq.4.21}$$

For 2 DOF system, Eq.4.20 gives two equations as:

$$\frac{d}{dt}\left(\frac{\partial T}{\partial \dot{V}}\right) - \left(\frac{\partial T}{\partial V}\right) + \left(\frac{\partial U}{\partial V}\right) - \left(\frac{\partial W_{ext}}{\partial V}\right) = 0 \quad \text{Eq.4.22}$$

And,

$$\frac{d}{dt}\left(\frac{\partial T}{\partial \dot{W}}\right) - \left(\frac{\partial T}{\partial W}\right) + \left(\frac{\partial U}{\partial W}\right) - \left(\frac{\partial W_{ext}}{\partial W}\right) = 0 \quad \text{Eq.4.23}$$

Now, Substituting Eq.4.18, 4.19 and 4.20 in Eq.4.22, we get,

$$\rho_s A\int_0^L \{\phi\}\{\phi\}^T\{\ddot{V}\}dx + m_d\{\phi\}_d\{\phi\}_d^T\{\ddot{V}\} + \rho_s I_s$$

$$\int_0^L \{\phi'\}\{\phi'\}^T\{\ddot{V}\}dx + \rho_d h I_d\{\phi'\}_d\{\phi'\}_d^T\{\ddot{V}\}$$

$$- 2\rho_s A\Omega\int_0^L \{\phi\}\{\phi\}^T\{\dot{W}\}dx - 2\rho_s I_s\Omega\int_0^L \{\phi'\}$$

$$\{\phi'\}^T\{\dot{W}\}dx - 2\,\rho_d h I_d\Omega\{\phi'\}_d\{\phi'\}_d^T\{\dot{W}\}$$

$$- 2\,m_d\Omega\{\phi\}_d\{\phi\}_d^T\{\dot{W}\} - \rho_s J_s\Omega\int_0^L \{\phi'\}\{\phi'\}^T\{$$

$$\dot{W}\}dx - \rho_d h J_d\Omega\{\phi'\}_d\{\phi'\}_d^T\{\dot{W}\} - \rho_s I_s\Omega^2\int_0^L \{\phi'\}$$

$$\{\phi'\}^T\{V\}dx - \rho_s A\Omega^2\int_0^L \{\phi\}\{\phi\}^T\{V\}dx$$

$$- \rho_d h I_d\Omega^2\{\phi'\}_d\{\phi'\}_d^T\{V\} - m_d\Omega^2\{\phi\}_d\{\phi\}_d^T\{V\}$$

$$+ EI_s\int_0^L \{\phi''\}\{\phi''\}^T\{V\}dx - F(t)\{\phi\}_d = 0$$

Eq.4.24

Likewise, substituting Eq.4.18, 4.19 and 4.20 in Eq.4.22, we get,

$$\rho_s A\int_0^L \{\phi\}\{\phi\}^T\{\ddot{W}\}dx + m_d\{\phi\}_d\{\phi\}_d^T\{\ddot{W}\} + \rho_s I_s$$
$$\int_0^L \{\phi'\}\{\phi'\}^T\{\ddot{W}\}dx + \rho_d h I_d\{\phi'\}_d\{\phi'\}_d^T\{\ddot{W}\}$$
$$+ 2\rho_s A\Omega\int_0^L \{\phi\}\{\phi\}^T\{\dot{V}\}dx + 2\rho_s I_s\Omega\int_0^L \{\phi'\}$$
$$\{\phi'\}^T\{\dot{V}\}dx + 2\rho_d h I_d\Omega\{\phi'\}_d\{\phi'\}_d^T\{\dot{V}\}$$
$$+ 2 m_d\Omega\{\phi\}_d\{\phi\}_d^T\{\dot{V}\} + \rho_s J_s\Omega\int_0^L \{\phi'\}\{\phi'\}^T\{\dot{V}\}$$
$$dx + \rho_d h J_d\Omega\{\phi'\}_d\{\phi'\}_d^T\{\dot{V}\} - \rho_s I_s\Omega^2\int_0^L \{\phi'\}$$
$$\{\phi'\}^T\{W\}dx - \rho_s A\Omega^2\int_0^L \{\phi\}\{\phi\}^T\{W\}dx$$
$$- \rho_d h I_d\Omega^2\{\phi'\}_d\{\phi'\}_d^T\{W\} - m_d\Omega^2\{\phi\}_d$$
$$\{\phi\}_d^T\{W\} + EI_s\int_0^L \{\phi''\}\{\phi''\}^T\{W\}dx = 0 \qquad \text{Eq.4.25}$$

Eq.4.24 and 4.25 are the governing equations for the rotodynamic system and can be represented as:

$$M_i\ddot{V} - C_i\dot{W} + K_i V = F_i \qquad \text{Eq.4.26}$$

$$M_i\ddot{W} + C_i\dot{V} + K_i W = 0 \qquad \text{Eq.4.27}$$

Where the equivalent parameters are as follows:

$$M_i = \rho_s A \int_0^L \{\phi\}\{\phi\}^T dx + m_d \{\phi\}_d \{\phi\}_d^T + \rho_s I_s \int_0^L \{\phi'\}\{\phi'\}^T dx + \rho_d h I_d \{\phi'\}_d \{\phi'\}_d^T \quad \text{Eq.4.28}$$

$$K_i = -\rho_s I_s \Omega^2 \int_0^L \{\phi'\}\{\phi'\}^T dx - \rho_s A \Omega^2 \int_0^L \{\phi\}\{\phi\}^T dx - \rho_d h I_d \Omega^2 \{\phi'\}_d \{\phi'\}_d^T - m_d \Omega^2 \{\phi\}_d \{\phi\}_d^T + E I_s \int_0^L \{\phi''\}\{\phi''\}^T dx \quad \text{Eq.4.29}$$

$$C_i = 2\rho_s A \Omega \int_0^L \{\phi\}\{\phi\}^T dx + 2\rho_s I_s \Omega \int_0^L \{\phi'\}\{\phi'\}^T dx + 2\rho_d h I_d \Omega \{\phi'\}_d \{\phi'\}_d^T + 2 m_d \Omega \{\phi\}_d \{\phi\}_d^T + \rho_s J_s \Omega \int_0^L \{\phi'\}\{\phi'\}^T dx + \rho_d h J_d \Omega \{\phi'\}_d \{\phi'\}_d^T \quad \text{Eq.4.30}$$

$$F_i = F(t)\{\phi\}_d \quad \text{Eq.4.31}$$

Now,

Coupled non-homogenous second order differential equations:

For first mode

$$M_1 \ddot{V} - C_1 \dot{W} + K_1 V = F_1 \quad \text{Eq.4.32}$$

$$M_1 \ddot{W} + C_1 \dot{V} + K_1 W = 0 \quad \text{Eq.4.33}$$

In matrix form,

$$\begin{bmatrix} M_1 & 0 \\ 0 & M_1 \end{bmatrix} \begin{bmatrix} \ddot{V} \\ \ddot{W} \end{bmatrix} + \begin{bmatrix} 0 & -C_1 \\ C_1 & 0 \end{bmatrix} \begin{bmatrix} \dot{V} \\ \dot{W} \end{bmatrix} + \begin{bmatrix} K_1 & 0 \\ 0 & K_1 \end{bmatrix} \begin{bmatrix} V \\ W \end{bmatrix} = \begin{bmatrix} F_1 \\ 0 \end{bmatrix} \quad \text{Eq.4.34}$$

For second mode

$$M_2 \ddot{V} - C_2 \dot{W} + K_2 V = F_2$$

$$M_2 \ddot{W} + C_2 \dot{V} + K_2 W = 0$$

For third mode

$$M_3 \ddot{V} - C_3 \dot{W} + K_3 V = F_3 \quad \text{Eq.4.35}$$

$$M_3 \ddot{W} + C_3 \dot{V} + K_3 W = 0 \quad \text{Eq.4.36}$$

4.3 Response from Mathematical Model

Writing governing second order differential equation in the system of ODE

Assume

$V = x_1$, $\dot{V} = \dot{x}_1 = x_2$, $\ddot{V} = \dot{x}_2$

$W = y_1$, $\dot{W} = \dot{y}_1 = y_2$, $\ddot{W} = \dot{y}_2$

System of ODEs are

$$\dot{x}_1 = x_2 \qquad \text{Eq.4.37}$$

$$\dot{x}_2 = -(K/M)\, x_1 + (C/M)\, y_2 + (F/M) \qquad \text{Eq.4.38}$$

$$\dot{y}_1 = y_2 \qquad \text{Eq.4.39}$$

$$\dot{y}_2 = -(C/M)\, x_2 - (K/M)\, y_1 \qquad \text{Eq.4.40}$$

Solving these four systems of ODE in MATLAB (Appendix B2 for starting and Appendix B3 for shutdown) we get the response,

Response in the direction of jet:

$$V = V_1\phi_1 + V_2\phi_2 + V_3\phi_3 \qquad \text{Eq.4.41}$$

4.4 Characteristic equation and shape functions

The governing equation of uniform Euler-Bernoulli beam can be written as:

$$\frac{\partial^2}{\partial x^2}\left(EI_s\frac{\partial^2 w}{\partial x^2}\right) + \rho A\frac{\partial^2 w}{\partial t^2} = f(x,t)$$ where f(x,t) is the forcing function Eq.4.42

For free vibration, f(x,t) = 0

Then governing equation becomes,

$$\frac{\partial^2}{\partial x^2}\left(EI_s\frac{\partial^2 w}{\partial x^2}\right) + \rho A\frac{\partial^2 w}{\partial t^2} = 0$$

For a uniform beam, it can be written as

$$c^2\frac{\partial^4 w}{\partial x^4} + \frac{\partial^2 w}{\partial t^2} = 0 \quad \text{where} \quad c = \sqrt{\frac{EI}{\rho A}}$$

The solution to free vibration, using method of separation of variables can be written as:

$w(x,t) = W(x)T(t)$

Then, the governing equation for uniform beam yields

$$\frac{c^2}{W(x)}\frac{d^4W(x)}{dx^4} = -\frac{1}{T(t)}\frac{d^2T(t)}{dt^2} = a = \omega^2$$ where $a = \omega^2$ is a positive constant

We can write,

$$\frac{d^2T(t)}{dt^2} - \omega^2 T(t) = 0$$

whose solution is given by $T(t) = A \cos \omega t + B \sin \omega t$

Further, the equation with the leftmost and rightmost terms can be written as

$$\frac{d^4W(x)}{dx^4} - \beta^4 W(x) = 0$$

Where $\beta^4 = \frac{\rho A \omega^2}{EI_s}$; ω = natural frequency of beam

The solution to this equation is assumed as $W(x) = Ce^{sx}$

Then from above equation,

$s^4 - \beta^4 = 0$ which gives the roots $s = \pm\beta, \pm i\beta$

Then solution W(x) can be written as

$W(x) = C_1e^{\beta x} + C_2e^{-\beta x} + C_3e^{i\beta x} + C_4e^{-i\beta x}$

This can be written as:

$W(x) = C_1\cos \beta x + C_2\sin \beta x + C_3\cosh \beta x + C_4\sinh \beta x$

or,

$W(x) = \phi(x) = C_1(\cos \beta x + \cosh \beta x) + C_2(\cos \beta x - \cosh \beta x) + C_3(\sin \beta x + \sinh \beta x) + C_4(\sin \beta x - \sinh \beta x)$ Eq.4.43

For a cantilever beam with end mass, the boundary conditions are:

$$w(0, t) = 0, \quad \frac{dw}{dt}(L, t) = 0$$

$$EI_s\frac{d^2w}{dx^2}(L, t) + I_{md}\frac{d^3w}{dx\,dt^2}(L, t) = 0, \quad EI_s\frac{d^3w}{dx^3}(L, t) - m_d\frac{d^2w}{dt^2}(L, t) = 0 \qquad \text{Eq.4.44}$$

(Rao, 2019)

Then, using $w(x,t) = W(x)T(t)$ in the four boundary condition equations in Eq.4.44, we obtain a system of equations with unknowns C_1, C_2,C_3 and C_4 with $C_1 = C_2 = 0$. For non-trivial solution for C_3 and C_4, determinants of the coefficients of the equations must equal zero which leads to the following characteristic:

$$1 + \cos \beta L \cosh \beta L + \left(\frac{\beta m_d}{\rho A}\right)(\cos \beta L \sinh \beta L - \sin \beta L \cosh \beta L) - \left(\frac{\beta^3 I_{md}}{\rho A}\right)(\cosh \beta L \sin \beta L + \sinh \beta L \cos \beta L) + \left(\frac{\beta^4 m_d I_{md}}{\rho^2 A^2}\right)(1 - \cos \beta L \cosh \beta L) = 0$$

Eq.4.45

It's eigen function is obtained as:

$$\phi(x) = (\cos \beta x - \cosh \beta x) + \frac{\sin \beta L - \sinh \beta L + \frac{\beta m_d}{\rho A}(\cos \beta L - \cosh \beta L)}{\cos \beta L + \cosh \beta L - \frac{\beta m_d}{\rho A}(\sin \beta L - \sinh \beta L)}(\sin \beta x - \sinh \beta x) \quad \text{Eq.4.46}$$

4.5 Simulation Setup

Beam material is added to the Engineering Data of the ANSYS analysis. The beam is modeled as a line body and meshing is done with 1mm elements.

Figure 4.3: Geometry of the model

Rigid bearing is added to one end of the shaft and point mass representing the disk is attached to the other end.

For the boundary condition, the vertex at the bearing is free to rotate about the longitudinal axis and free to move in the transverse directions while the remaining degrees of freedom are constrained.

Modal analysis is done to find the modes of vibration followed by the transient structural analysis. Time step for the transient analysis is chosen as 0.001s. Transient impact force is applied in the transverse direction at the free end vertex where the point mass is located. Transient rotational velocity is also applied to the beam.

CHAPTER FIVE: RESULTS AND DISCUSSION

5.1 Equivalent Parameters

Solving Eq.4.45 for given system parameters, we obtain values of βL for the first three modes of vibration as: 0.57680, 1.12511 and 4.74416 respectively.

Then, using Eq.4.46, the shape functions for the first three modes of vibration are:

For first mode,

ϕ_1 = cos(0.57680x/L)-cosh(0.57680x/L)-1.27460(sin(0.57680x/L)-sinh(0.57680x/L))

For second mode,

ϕ_2 = cos(1.12511x/L)-cosh(1.12511x/L)-2.21274(sin(1.12511x/L)-sinh(1.12511x/L))

For third mode,

ϕ_3 = cos(4.74416x/L)-cosh(4.74416x/L)-0.98291(sin(4.74416x/L)-sinh(4.74416x/L))

Equations Eq.4.28 to 4.31 are modeled in MATLAB using the above shape functions and equivalent mass, damping coefficient, stiffness and forcing vector for modes 1, 2 and 3 are evaluated (see Appendix B1).

Table 5.1 Equivalent parameters

For first mode	For second mode	For third mode
ϕ_1	ϕ_2	ϕ_3
M_1= 0.67585 kg	M_2= 0.52879 kg	M_3= 0.66630 kg
C_1 = 1.35236Ω Ns/m	C_2=1.05868Ω Ns/m	C_3 = 1.43657Ω Ns/m
K_1 = 2247630.20231 - 0.67585Ω^2 N/m	K_2 = 40923956.49522 - 0.52878 N/m	K_3 = 5793877930.31206 - 0.66630Ω^2 N/m
F_1 = -0.25126 F(t)	F_2 = -0.21901 F(t)	F_3 = 0.02375 F(t)

5.2 Response during Startup

Figure 5.1 shows the response of a cantilever shaft-disk system during startup for the first mode of vibration. For the first mode, the maximum deflection is around 5.5μm in the direction of the jet. The deflection reaches its peak value as the startup is complete. After completion of the startup operation, the deflection remains constant

as full jet impact load is continuously acting on the system. Figure 5.2 shows the zoomed in view of the response where oscillating deflection represents the vibration.

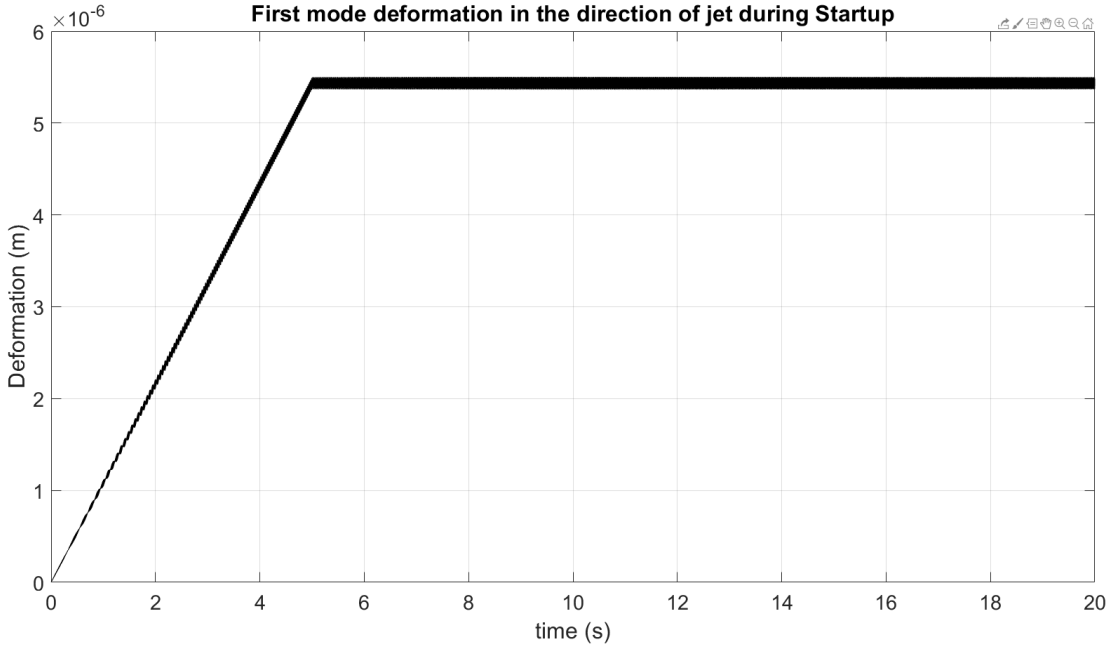

Figure 5.1 First mode response of cantilever shaft-disk during startup

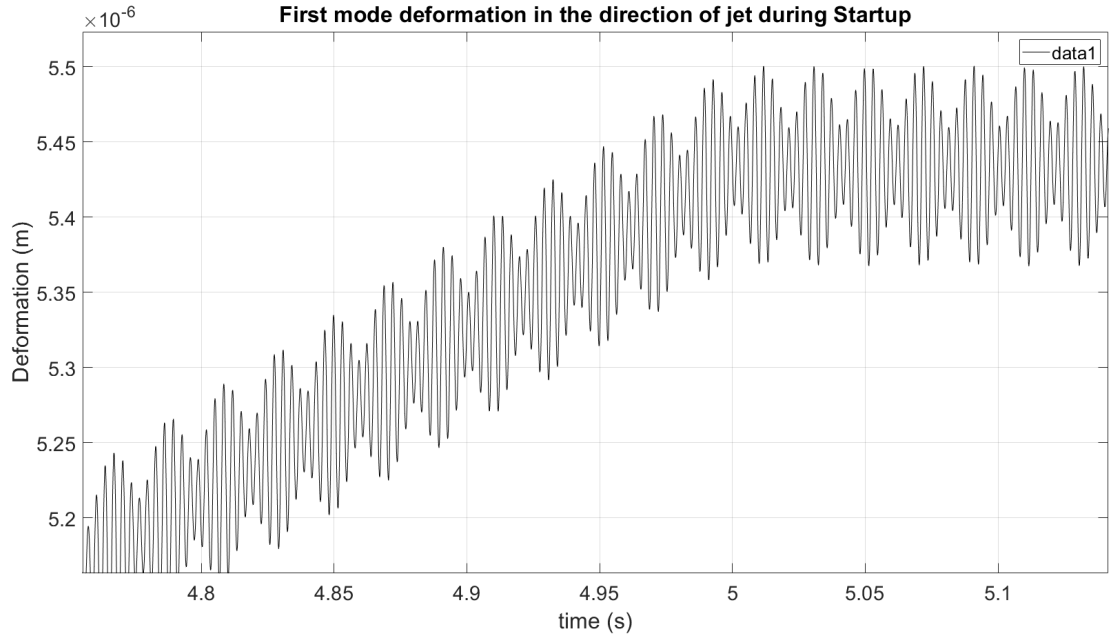

Figure 5.2 Zoomed-in view of first mode response during startup

Figure 5.3 shows the response of a cantilever shaft-disk system during startup for the second mode of vibration. Here, the maximum deflection is around 0.3μm in the direction of the jet.

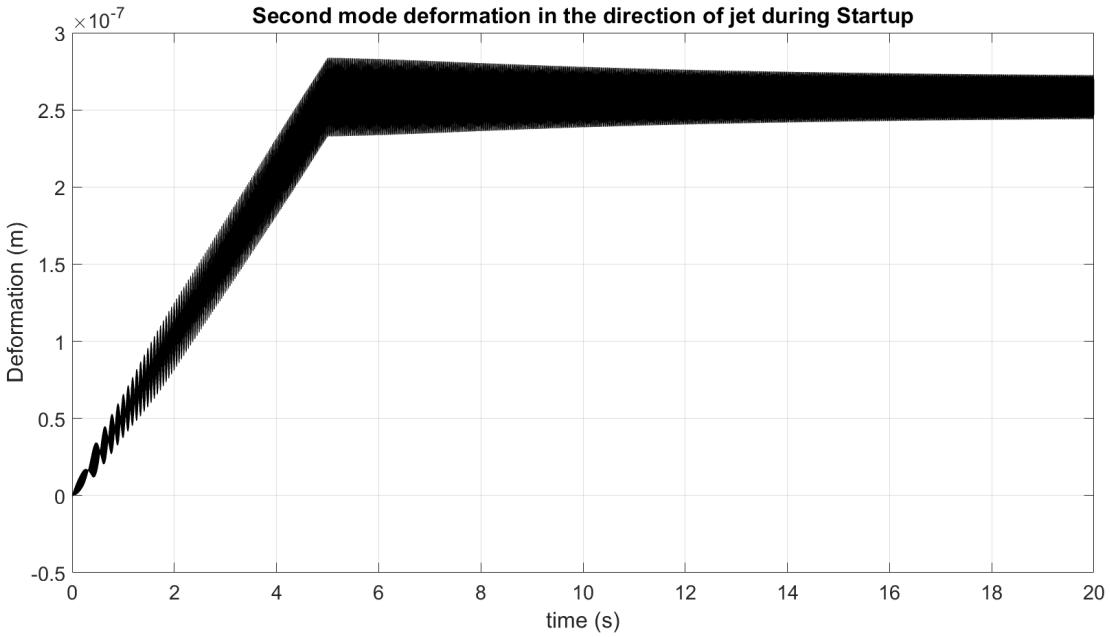

Figure 5.3 Second mode response of cantilever shaft-disk during startup

Figure 5.4 shows the response of a cantilever shaft-disk system during startup for the third mode of vibration.

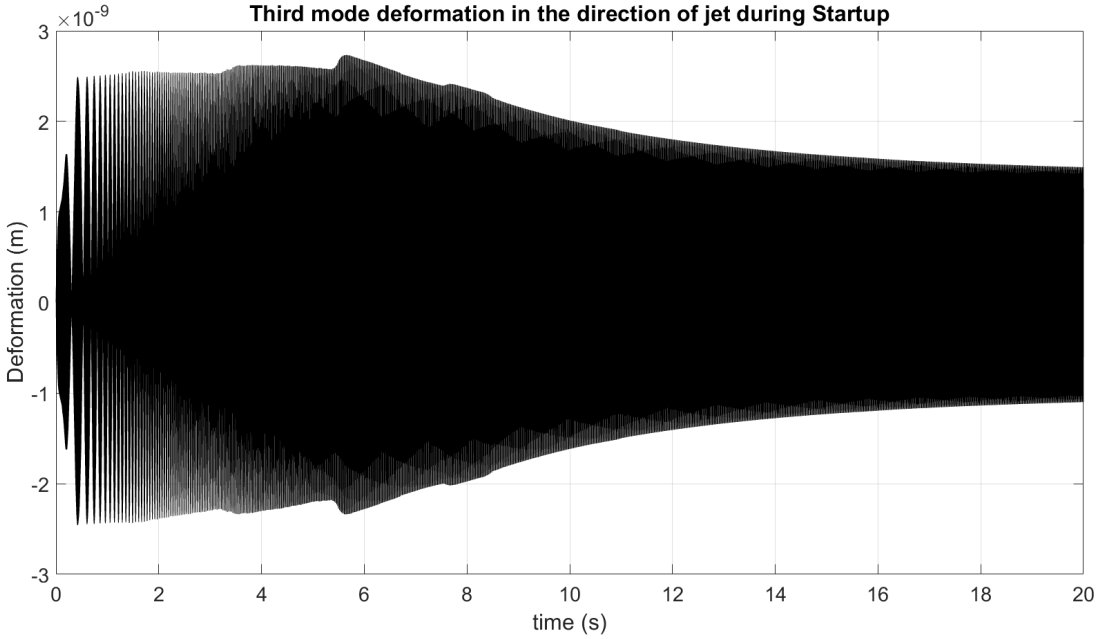

Figure 5.4 Third mode response of cantilever shaft-disk during startup

As compared to the first and second modes, the deflection in the third mode of vibration is negligible. So the total response of the system is obtained as the sum of deflections in the first and second modes of vibration.

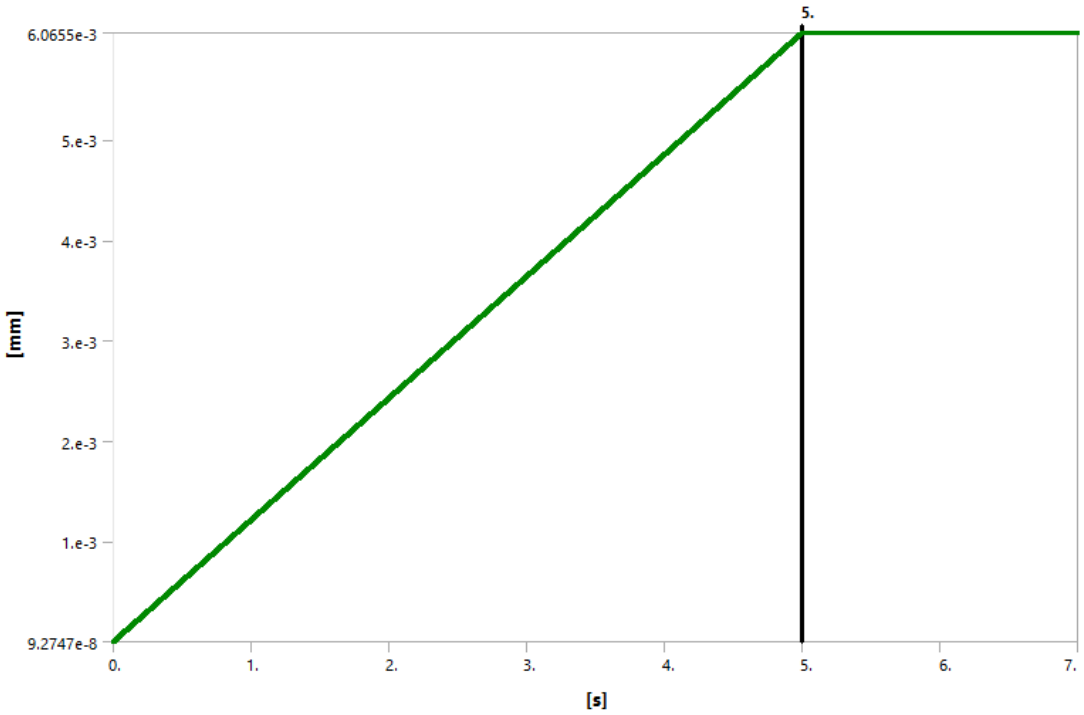

Figure 5.5 Startup response of cantilever shaft-disk from ANSYS simulation

Figure 5.5 shows the response as obtained from the simulation. The maximum deflection of the shaft-disk system is around 6.1μm during startup at the end of the startup period. After the starting period, the excitation force is constant and continuously acting on the system and so is the deflection of the system.

5.3 Response during Shutdown

Figure 5.6 shows the response of a cantilever shaft-disk system during shutdown for the first mode of vibration. For the first mode, the maximum deflection is around 10.5 μm in the direction of the jet. The deflection has peak value at the beginning of the shutdown operation. After completion of the shutdown operation, the mean deflection is zero.

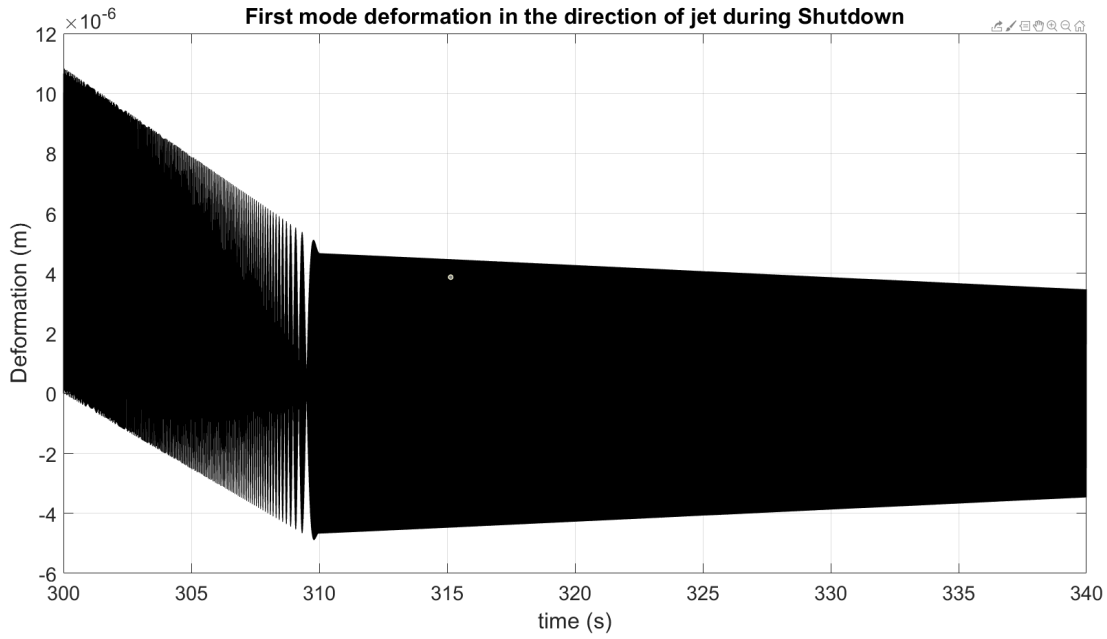

Figure 5.6 First mode response of cantilever shaft-disk during shutdown

Figure 5.7 shows the response of a cantilever shaft-disk system during shutdown for the second mode of vibration. For the second mode, the maximum deflection is around 0.5 μm in the direction of the jet. Again, the deflection has peak value at the beginning of the shutdown operation. After completion of the shutdown operation, the mean deflection is zero.

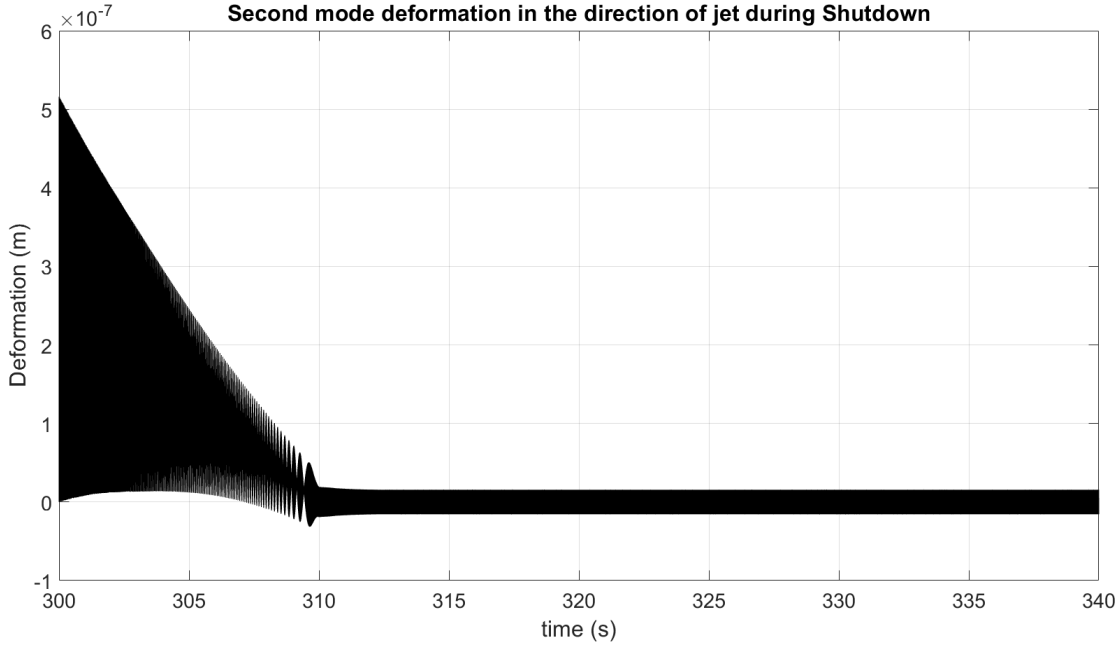

Figure 5.7 Second mode response of cantilever shaft-disk during shutdown

Figure 5.8 shows the response of a cantilever shaft-disk system during shutdown for the third mode of vibration.

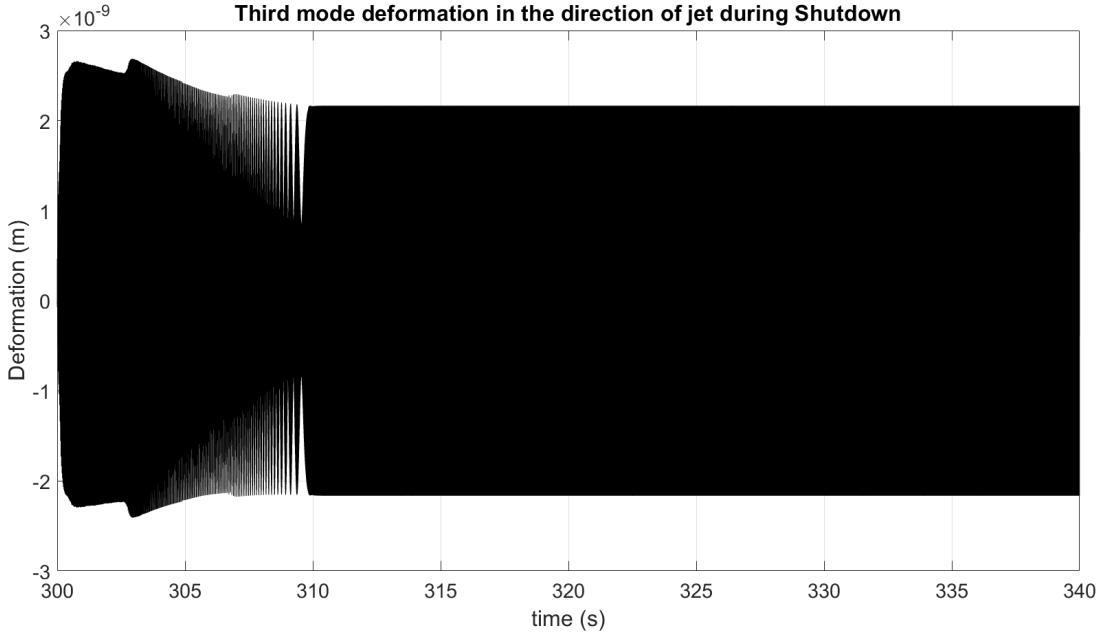

Figure 5.8 Third mode response of cantilever shaft-disk during shutdown

As compared to the first and second modes, the deflection in the third mode of vibration is negligible. So the total response of the system is obtained as the sum of deflections in the first and second modes of vibration for the shutdown as well.

Figure 5.9 shows the shutdown response as obtained from the simulation. The maximum deflection of the shaft is around 11.5μm during shutdown. After the shutdown period, the excitation force goes to zero and so does the deflection of the system.

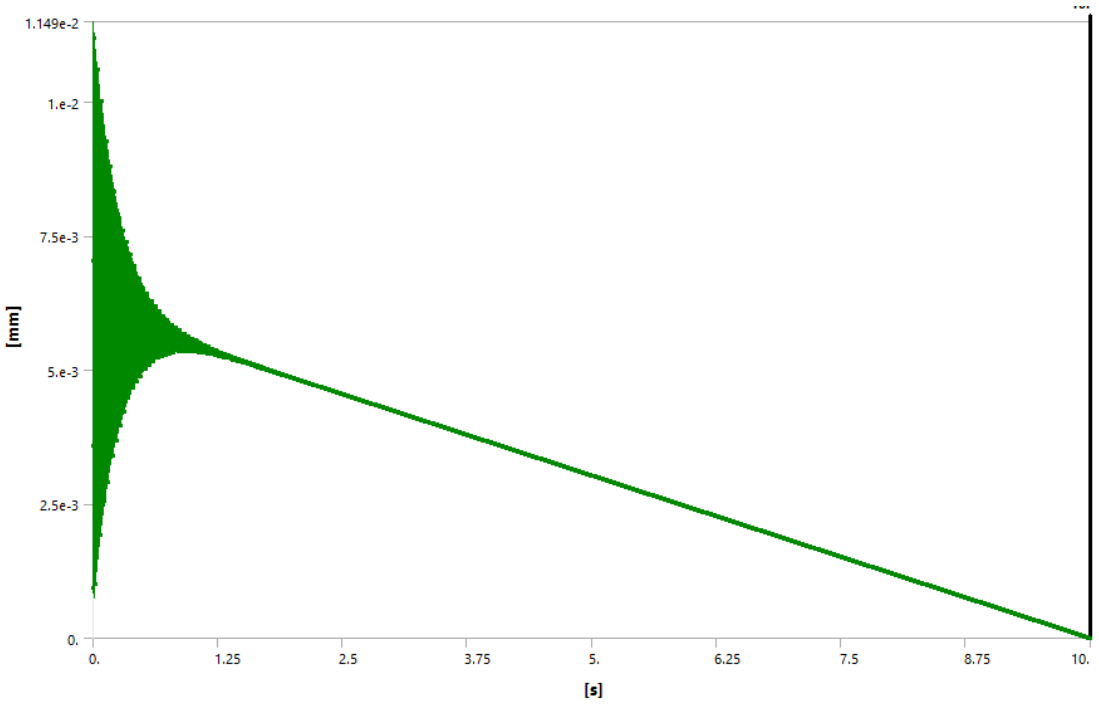

Figure 5.9 Shutdown response of cantilever shaft-disk from ANSYS simulation

CHAPTER SIX: CONCLUSIONS AND RECOMMENDATIONS

6.1 Conclusions

The transient response of the cantilever shaft-disk system based on the data from the selected Pelton turbine unit is thus obtained. The maximum deflection that can be expected during startup and shutdown is obtained by summing the deflections for the first two modes since the third mode has negligible deflection.

- The maximum deflection obtained from the mathematical model during startup is around 5.8μm and during shutdown is around 11μm for the given choice of pelton turbine representing the cantilever shaft-disk system.
- The maximum deflection obtained from the simulation in ANSYS during startup is around 6.1μm and during shutdown is around 11.5μm.
- The deflection variation between mathematical model and simulated result is 5.2% for startup whereas it is 4.5% for shutdown.

6.2 Recommendations

This work can be expanded following the recommendations given below:

- The force of the impact jet acting on the disk is assumed linear in this work. It would be best to incorporate actual function representing the force of the jet during transient periods.
- The simplified disk can be replaced with actual pelton turbine geometry with buckets for analysis of transient impact response of the pelton turbine.
- Response to multiple impact jets can be studied.
- Analysis can be done for a flexible disk as well as flexible bearing.

REFERENCES

Beer, F. P., DeWolf, J. T., Mazurek, D., & Johnston, E. R. (2011). *Mechanics of Materials*. McGraw-Hill Education.

Bhandari, R., & Luintel, M. C. (2019). Dynamic Response of Overhung Pelton Turbine Unit for Forced Vibration. *Proceedings of IOE Graduate Conference*.

Coutu, A., Dörfler, P., & Sick, M. (2013). *Flow-Induced Pulsation and Vibration in Hydroelectric Machinery: Engineer's Guidebook for Planning, Design and Troubleshooting*. Springer London.

Egusquiza, M., Valentin, D., Presas, A., & Egusquiza, E. (2021). Transient Analysis of Pelton Turbine Prototypes. *IOP Conference Series: Earth and Environmental Science*, *774*. 10.1088/1755-1315/774/1/012120

Egusquiza, M., Valero, C., Presas, A., Valentin, D., & Egusquiza, E. (2019). Experimental investigation on the dynamic response of Pelton Runners. *IOP Conf. Ser.: Earth Environ. Sci.*, *240*(2). 10.1088/1755-1315/240/2/022062

Jirel, B., Luintel, M. C., & Shakya, P. R. (2021). Dynamic Response of Overhung Pelton Turbine Unit under Rotating Unbalance. *Proceedings of 9th IOE Graduate Conference*, *9*, 147-154.

Karki, S., Luintel, M. C., & Poudel, L. (2017). Dynamic Response of Pelton Turbine Unit for Forced Vibration. *Proceedings of IOE Graduate Conference*, *5*, 509-517.

Khader, N., Atoum, A., & Al-Qaisia, A. (2007). Theoretical and Experimental Modal Analysis of Multiple Flexible Disk-Flexible Shaft System.

Khanlo, H. M., Ghayour, M., & Ziaei-Rad, S. (2011). Chaotic vibration analysis of rotating, flexible, continuous shaft-disk system with a rub-impact between the disk and the stator. *Commun Nonlinear Sci Numer Simulat*, *16*, 566-582. 10.1016/j.cnsns.2010.04.011

Luintel, M. C. (2019). Dynamic Modelling and Response of a Pelton Turbine Unit. 10.13140/RG.2.2.34011.82728

Luintel, M. C. (2021). Development of Polynomial Mode Shape Functions for Continuous Shafts with Different End Conditions. *Journal of the Institute of Engineering*, *16*(1), 151-161.

Luintel, M. C., & Bajracharya, T. R. (2019). Dynamic response of a Pelton turbine shaft under the impact of water jet. *Journal of Computational and Applied Research in Mechanical Engineering*, *10*(1), 73-84.

Motra, L., & Luintel, M. C. (2017). Free Vibration Analysis of Selected Pelton Turbine using Dynamic Approach. *IOE Graduate Conference*.

Rajak, A., Shrestha, P., Rijal, M., Pudasaini, B., & Luintel, M. C. (2014). Dynamic Analysis of Pelton Turbine and Assembly. *Proceedings of IOE Graduate Conference*.

Rao, S. S. (2017). *Mechanical Vibrations*. Pearson Education, Incorporated.

Rao, S. S. (2019). *Vibration of Continuous Systems*. John Wiley & Sons, Inc.

Zeng, Y., Zhang, L. X., Zhang, C. L., & Yu, F. R. (2012). Hamiltonian model of shafting lateral vibration for hydro turbine generating sets. *IOP Conf. Series: Earth and Environmental Science*, *15*. 10.1088/1755-1315/15/4/042004

APPENDIX A

Parameters	Values
Density of water (ρ_w)	1000 kg/m^3
Pitch Circle Diameter of Runner (D_R)	155 mm
Rated RPM (N)	1500 rpm
Diameter of shaft (d_s)	32 mm
Cross section area of shaft (A)	0.0008042 m^2
Area polar moment of inertia of shaft (J_s)	5.1472×10-8 m^4
Area moment of inertia of shaft about transverse axes (I_s)	1.0294×10-7 m^4
Area polar moment of inertia of disk (J_d)	0.5527×10-4 m^4
Area moment of inertia of disk about transverse axes (I_d)	0.11053×10-3 m^4
Length of shaft (L')	519 mm
Material of shaft	Mild steel
Density of shaft material (ρ_s)	7860 kg/m^3
Density of disk material (ρ_d)	8550 kg/m^3
Young's Modulus of Elasticity of shaft (E)	202 GPa
Mass of rotating runner (m_d)	10.564 kg
Thickness of runner (h)	0.035 m
Mass polar moment of inertia of disk about x-x axis (J_{md})	0.0334 kgm^2
Mass moment of inertia of disk about y-y or z-z axis (I_{md})	0.0206 kgm^2
Nominal spin speed ($\Omega = 2\pi N/60$)	157.07 rad/s

(Luintel, 2019)

APPENDIX B

1. MATLAB program for Equivalent System Parameters

```
clc
clear
syms x w F; % w is shaft rotational speed
rhoDisk = 8550; % Disk density
widthDisk = 0.035; % Disk thickness
I_Disk = 0.00005527; % Disk area moment of inertia about transverse axes
J_Disk = 0.00011053; % Disk polar moment of inertia
massDisk = 10.564; % Disk mass
rhoShaft = 7860; % Shaft density
E_Shaft = 2.02*10^11; %Shaft Modulus of Elasticity
areaShaft = 0.0008042; % Shaft cross section area
L = 0.097; % Shaft length
I_Shaft = 5.1472*10^-8; % Shaft area moment of inertia about transverse axes
J_Shaft = 1.0284*10^-7; % Shaft polar moment of inertia

% Shape function
phi=cos(1.12511*x/L)-cosh(1.12511*x/L)-2.21274*(sin(1.12511*x/L)-sinh(1.12511*
x/L));
d_phi=(diff(phi,1));
% Shape function for disk
phi_disk=subs(phi,x,L);
d_phi_disk=diff(phi_disk,1);
dd_phi=diff(phi,2);
% Equivalent mass
Meq=vpa(rhoShaft*areaShaft*(int(phi^2,0,L))+rhoShaft*I_Shaft*(int(d_phi^2,0,L))+
massDisk*phi_disk^2+rhoDisk*widthDisk*I_Disk*d_phi_disk^2)
% Equivalent damping coefficient
Ceq=vpa(2*rhoShaft*areaShaft*w*(int(phi^2,0,L))+2*rhoShaft*I_Shaft*w*(int(d_ph
i^2,0,L))+2*massDisk*w*phi_disk^2+2*rhoDisk*widthDisk*I_Disk*w*d_phi_disk^
2+rhoShaft*J_Shaft*w*(int(d_phi^2,0,L))+rhoDisk*widthDisk*J_Disk*w*d_phi_dis
k^2)
% Equivalent stiffness
```

```
Keq=vpa(-rhoShaft*areaShaft*w^2*(int(phi^2,0,L))-rhoShaft*I_Shaft*w^2*(int(d_p
hi^2,0,L))-massDisk*w^2*phi_disk^2-rhoDisk*widthDisk*I_Disk*w^2*d_phi_disk^
2+E_Shaft*I_Shaft*int(dd_phi^2,0,L))
% Equivalent force
Feq=vpa(F*phi_disk)
```

2. MATLAB program for Startup

```
clc
clear
duration=[0 20]; % Duration considered for result is 20 sec
Y0=[0 0 0 0]; % Initial conditions for the ODE system
tolerance = odeset('RelTol',1e-5);
[t_out,Y_out] = ode45(@sys_of_ODEs,duration,Y0,tolerance);
v=Y_out(:,1); % deflection in jet direction
% Plot deflection in jet direction
plot(t_out,v,'k');
set(gca,'fontsize', 22)
set(gcf,'color','w');
grid on
title('Third mode deformation in the direction of jet during Startup');
xlabel('time (s)');
ylabel('Deformation (m)');

function ODEs = sys_of_ODEs(t,Y)
 x1=Y(1); x2=Y(2); y1=Y(3); y2=Y(4);
  % System parameters
 M=0.55932; % Equivalent mass of the system
 Fj=193*-0.2286; % Equivalent impact force
 t0=5; % Duration of complete startup
 w_nom=157.07; % Nominal speed of shaft
  % Force change during startup
 F= Fj/t0*t*(1-heaviside(t-t0)) + Fj* heaviside(t-t0);
  % Rotational speed change during startup
 w= w_nom/t0*t*(1-heaviside(t-t0))+ w_nom* heaviside(t-t0);
```

```
 % Equivalent stiffness
K=1957802.62 - 0.559*w^2;
 % Damping coefficient
C= 1.119*w;
 % System of second order differential equations
% M1*diff(v,t,2)-C1*diff(w,t)+K1*v=F1 & M1*diff(w,t,2)+C1*diff(v,t)+K1*w=0
% Assume v=x1,dv=x2,w=y1,dw=y2
dx1=x2;
dx2=-K/M*x1+C/M*y2+F/M;
dy1=y2;
dy2=-C/M*x2-K/M*y1;
 % System of ODEs
ODEs=[dx1;dx2;dy1;dy2];
end
```

3. MATLAB program for Shutdown

```
clc
clear
duration=[300 340]; % Duration considered for result is 40 sec
Y0=[0 0 0 0]; % Initial conditions for the ODE system
tolerance = odeset('RelTol',1e-5);
[t_out,Y_out] = ode45(@sys_of_ODEs,duration,Y0,tolerance);
v=Y_out(:,1); % deflection in jet direction
% Plot deflection in jet direction
plot(t_out,v,'k');
set(gca,'fontsize', 22)
set(gcf,'color','w');
grid on
title('Third mode deformation in the direction of jet during Startup');
xlabel('time (s)');
ylabel('Deformation (m)');

function ODEs = sys_of_ODEs(t,Y)
 x1=Y(1); x2=Y(2); y1=Y(3); y2=Y(4);
```

```
 % System parameters
M=0.55932; % Equivalent mass of the system
Fj=193*-0.2286; % Equivalent impact force
ta=300; %Shutdown beginning time
ts=10; % Duration of complete shutdown
w_nom=157.07; % Nominal speed of shaft
% Force change during startup
F= -Fj/ts*(t-(ta+ts))*(1-heaviside(t-(ta+ts)));
% Rotational speed change during startup
w= -w_nom/ts*(t-(ta+ts))*(1-heaviside(t-(ta+ts)));
% Equivalent stiffness
K=1957802.62 - 0.559*w^2;
% Damping coefficient
C= 1.119*w;
% System of second order differential equations
% M1*diff(v,t,2)-C1*diff(w,t)+K1*v=F1 & M1*diff(w,t,2)+C1*diff(v,t)+K1*w=0
% Assume v=x1,dv=x2,w=y1,dw=y2
dx1=x2;
dx2=-K/M*x1+C/M*y2+F/M;
dy1=y2;
dy2=-C/M*x2-K/M*y1;
% System of ODEs
ODEs=[dx1;dx2;dy1;dy2];
end
```

obtain the response of a cantilever shaft-disk during transient stages of startup and shutdown with a mathematical model and to compare the results with simulation.

ORIGINALITY REPORT

7%
SIMILARITY INDEX

PRIMARY SOURCES

1	elibrary.tucl.edu.np Internet	39 words — 1%
2	SHEU, H.C.. "A LUMPED MASS MODEL FOR PARAMETRIC INSTABILITY ANALYSIS OF CANTILEVER SHAFT-DISK SYSTEMS", Journal of Sound and Vibration, 20000706 Crossref	36 words — 1%
3	www.coursehero.com Internet	31 words — 1%
4	www.grin.com Internet	25 words — 1%
5	H.M. Khanlo, M. Ghayour, S. Ziaei-Rad. "Chaotic vibration analysis of rotating, flexible, continuous shaft-disk system with a rub-impact between the disk and the stator", Communications in Nonlinear Science and Numerical Simulation, 2011 Crossref	24 words — 1%
6	ir.kiu.ac.ug Internet	15 words — < 1%

7	prism.ucalgary.ca Internet	14 words — < 1%
8	Zhang, Ye. "Piezoelectric Based Energy Harvesting on Low Frequency Vibrations of Civil Infrastructures", Louisiana State University and Agricultural & Mechanical College, 2022 ProQuest	10 words — < 1%
9	documentserver.uhasselt.be Internet	9 words — < 1%
10	utpedia.utp.edu.my Internet	9 words — < 1%
11	B. F. Klochkov, V. G. Muramovich. "Calculation of working loads and evaluation of the service life for icebreaker stern bearings", Journal of Engineering Physics and Thermophysics, 1999 Crossref	8 words — < 1%
12	Houxin She, Chaofeng Li, Qiansheng Tang, Bangchun Wen. "Influence mechanism of disk position and flexibility on natural frequencies and critical speeds of a shaft-disk-blade unit", Journal of Sound and Vibration, 2020 Crossref	8 words — < 1%
13	open.uct.ac.za Internet	8 words — < 1%
14	repository.riteh.uniri.hr Internet	8 words — < 1%
15	Prajapati, Seezan. "Numerical Investigation of Power Generated by Turbine Farms.", University of Cincinnati, 2020	6 words — < 1%

EXCLUDE QUOTES	ON	EXCLUDE SOURCES	< 6 WORDS
EXCLUDE BIBLIOGRAPHY	ON	EXCLUDE MATCHES	< 6 WORDS

IOE Graduate Conference
[Placeholder for Publication Information]

Vibration analysis of cantilever shaft-disk system for transient response to water impact

Bidhan Pandey, Prof. Dr. Mahesh Chandra Luintel

Department of Mechanical and Aesospace Engineering, Pulchowk Campus, IOE, Tribhuvan University, Nepal

Abstract

Engineering applications like hydraulic turbine, axial compressor and turbine engine systems are all examples of Shaft-disk systems. Analysis of simplified shaft-disk systems representing such applications can be useful in understanding the dynamic response of those applications. Start-up transients are one of the most critical operating conditions in hydraulic turbines. In this research, transient response analysis is done for a cantilever shaft-disk system which can be used to understand the behavior of application like a cantilever Pelton turbine. The study involves developing a mathematical model for the cantilever shaft-disk system. Excitation force used is based on the transient impact jet force that would act on a Pelton turbine during startup and shutdown. Vibration response of the excitation force is evaluated by solving the governing equations from the mathematical model with the defined excitation force. Vibration amplitudes are obtained for the first three modes of vibration for both cases of startup and shutdown.

Keywords

Transient response, Pelton turbine, Modes of vibration

1. Introduction

Engineering applications like hydraulic turbine, axial compressor and turbine engine systems are all examples of Shaft-disk systems. Water impact on the disk of a cantilever shaft-disk system can represent a cantilever Pelton turbine and thus analysis on such a system can be used to estimate performance of a Pelton turbine. Due to their high operating speed and high-performance requirements, vibrational analysis is an important aspect in the design of these applications. A coupled vibrational study of the shaft-disk system is essential to get the overall response of the system which can be used to avoid any undesirable deformation or structural damage.

Startup transient is considered as a critical operation in hydraulic turbines. The speed of the turbines vary during startup as it goes from rest to the operating speed. Likewise, during shutdown, the speed varied from operating speed to zero. These operating conditions mark the cases of transient loading and are the subjects of study for this thesis for a cantilever shaft-disk system. The response of a shaft-disk system such as a Pelton turbine depends on the operating parameters as well as its components. Researchers have modeled rotodynamic systems as shaft-disk systems to investigate various aspects of those systems. Figure 1 shows a cantilever shaft-disk system whose vibrational analysis is done in this work.

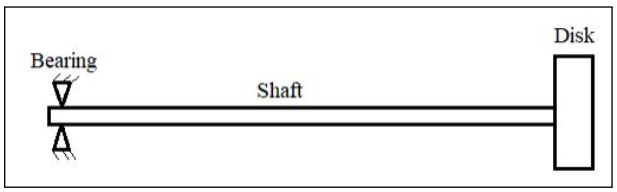

Figure 1: Shaft-disk representation of a cantilever Pelton turbine

2. Mathematical Model Development

Let us consider a rigid disk attached to a flexible shaft as shown in figure 1. Water will impact the disk in the y-direction. The transverse displacements of points on the shaft be v(x,t) and w(x,t) in the horizontal and vertical directions respectively. The kinematic equations of the shaft and disk [1] are given below. Angular velocity of shaft:

$$\omega_s = \Omega \vec{i} \tag{1}$$

Velocity of points on neutral axis of the shaft:

$$v_s = (\dot{v} - \Omega w)\vec{j} + (\dot{w} + \Omega v)\vec{k} \tag{2}$$

Angular velocity of the disk:

$$\omega_d = (\Omega + v'\dot{w}')\vec{i} + (-\Omega v' - \dot{w}')\vec{j} + (-\Omega w' + \dot{v}')\vec{k} \tag{3}$$

2.1 Energy of the System

Kinetic energy of rotating shaft:

$$\begin{aligned} T_s &= \frac{1}{2}\rho_s A \int_0^L [(\dot{v} - \Omega w)^2 + (\dot{w} + \Omega v)^2]\, dx \\ &+ \frac{1}{2}\rho_s J_s \int_0^L (\Omega + v'\dot{w}')^2\, dx \\ &+ \frac{1}{2}\rho_s I_s \int_0^L [(-\Omega v' - \dot{w}')^2 + (-\Omega w' + \dot{v}')^2]\, dx \end{aligned} \tag{4}$$

Potential energy of rotating shaft:

$$U_s = \frac{1}{2} E I_s \int_0^L [v''^2 + w''^2]\, dx \tag{5}$$

Kinetic energy of the disk:

$$\begin{aligned} T_s &= [\frac{1}{2} M_d[(\dot{v} - \Omega w)^2 + (\dot{w} + \Omega v)^2] \\ &+ \frac{1}{2}\rho_d h J_d (\Omega + v'\dot{w}')^2 \\ &+ \frac{1}{2}\rho_d h I_d [(-\Omega v' - \dot{w}')^2 + (-\Omega w' + \dot{v}')^2]]|_{x=L} \end{aligned} \tag{6}$$

Disk is assumed as a rigid body and hence its potential energy is zero.

$$U_d = 0 \tag{7}$$

2.2 Excitation force

As the excitation force for the shaft-disk system, impact of water jet on the pelton turbines will be taken. The speed of the turbine varies during the startup and shutdown. [2] has evaluated the jet force for the same pelton turbine system used in this research as: Fj = 193 N

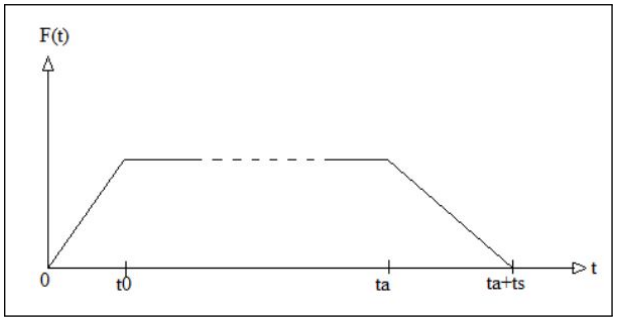

Figure 2: Startup and shutdown excitation

Excitation force is assumed to be linear during transient stages as shown in Figure 2. Startup excitation force:

$$F = (F_j/t_0)t(1 - u(t - t_0)) + F_j u(t - t_0) \tag{8}$$

Shutdown excitation force:

$$F = (F_j - (F_j/t_s)(t - t_a))(u(t - t_a) - u(t - (t_a + t_s)) \tag{9}$$

Startup time is taken as 5 seconds and shutdown time is taken as 10 seconds for this analysis. Work done by the impact jet:

$$W_{ext} = F(t)v|_{x=L} \tag{10}$$

2.3 Equivalent Parameters

From assumed mode method, displacement variables defined as product of spatial and time dependent functions are:

$$\begin{aligned} v &= \phi(x)^T V(t) \\ w &= \phi(x)^T W(t) \end{aligned} \tag{11}$$

Lagrange equation for getting the equations of motion is:

$$\frac{d}{dt}(\frac{\partial T}{\partial \dot{q}}) - \frac{\partial T}{\partial q} + \frac{\partial U}{\partial \dot{q}} - \frac{\partial W_{ext}}{\partial \dot{q}} = 0 \tag{12}$$

where q represents each degree of freedom. Combining equations (4) through (11), the governing equation of rotodynamic system can be written as:

$$M_i\ddot{V} - C_i\dot{W} + K_i V = F_i \tag{13}$$

$$M_i\ddot{W} + C_i\dot{V} + K_i W = 0 \tag{14}$$

Where

$$M_i = \rho_s A \int_0^L \phi\phi^T dx + \rho_s I_s \int_0^L \phi'\phi'^T dx + M_d[\phi_d\phi_d^T] + \rho_d h I_d[\phi_d'\phi_d'^T] \quad (15)$$

$$C_i = 2\rho_s A\Omega \int_0^L \phi\phi^T dx + 2\rho_s I_s\Omega \int_0^L \phi'\phi'^T dx + 2M_d\Omega[\phi_d\phi_d^T] + 2\rho_d h I_d\Omega[\phi_d'\phi_d'^T] + \rho_s J_s\Omega \int_0^L \phi'\phi'^T dx + \rho_d h J_d\Omega[\phi_d'\phi_d'^T] \quad (16)$$

$$K_i = -\rho_s A\Omega^2 \int_0^L \phi\phi^T dx - \rho_s I_s\Omega^2 \int_0^L \phi'\phi'^T dx + -M_d\Omega^2[\phi_d\phi_d^T] - \rho_d h I_d\Omega^2[\phi_d'\phi_d'^T] + EI_s \int_0^L \phi''\phi''^T dx \quad (17)$$

$$F_i = F(t)\phi_d \quad (18)$$

Rewriting second order differential equations (13) and (14) in the system of ordinary differential equations, assume,

$$V = x_1, \dot{V} = \dot{x_1} = x_2, \ddot{V} = \dot{x_2}$$

$$W = y_1, \dot{W} = \dot{y_1} = y_2, \ddot{W} = \dot{y_2}$$

System of ordinary differential equations:

$$\dot{x_1} = x_2$$

$$\dot{x_2} = -(K/M)x_1 + (C/M)y_2 + (F/M)$$

$$\dot{y_1} = y_2$$

$$\dot{y} = -(C/M)x_2 - (K/M)y_1 \quad (19)$$

Solving these equations, we get the response in the direction of jet considering three modes of vibration as:

$$V = V_1\phi_1 + v_2\phi_2 + V_3\phi_3$$

2.4 Characteristic equation and shape functions

The governing equation of uniform Euler-Bernoulli beam can be written as:

$$\frac{\partial^2}{\partial x^2}(EI_s\frac{\partial^2 v}{\partial x^2}) + \rho_s A_s\frac{\partial^2 v}{\partial t^2} = f(x,t) \quad (20)$$

For a cantilever beam with end mass, the boundary conditions are:

$$v(0,t) = 0, \frac{dv}{dt}(L,t) = 0$$

$$EI_s\frac{\partial^2 v}{\partial x^2}(L,t) + I_{md}\frac{\partial^3 v}{\partial x\partial t^2}(L,t) = 0$$

$$EI_s\frac{\partial^3 v}{\partial x^3}(L,t) - M_d\frac{\partial^2 v}{\partial t^2}(L,t) = 0 \quad (21)$$

[3] Solving the boundary value problem Equations (20) and (21), characteristic equation of different eigen value problem for the cantilever uniform beam with end mass is derived as:

$$1 + cos\beta L cosh\beta L + \frac{\beta M_d}{\rho_s A_s}(cos\beta L sinh\beta L - sin\beta L cosh\beta L) - \frac{\beta^3 I_{md}}{\rho_s A_s}(cosh\beta L sin\beta L + sinh\beta L cos\beta L) + \frac{\beta^4 M_d I_{md}}{\rho_s^2 A_s^2}(1 - cos\beta L cosh\beta L) = 0 \quad (22)$$

where

$$\beta^4 = \frac{\rho_s A_s\omega^2}{EI_s}; \omega = natural\,frequency$$

The obtained eigen function is:

$$\phi(x) = (cos\beta x - cosh\beta x) + \frac{sin\beta L - sinh\beta L + \frac{\beta M_d}{\rho_s A_s}(cos\beta L - cosh\beta L)}{cos\beta L + cosh\beta L - \frac{\beta M_d}{\rho_s A_s}(sin\beta L - sinh\beta L)}X (sin\beta x - sinh\beta x) \quad (23)$$

Table 1 shows the parameters of a simply supported pelton turbine used as the reference for this work. The length of the equivalent cantilever pelton turbine is obtained by equating the static deflection functions [4] a simply supported and a cantilever shaft with equal load and the length obtained is 97mm.

Table 1: Parameters for the shaft-disk model

Parameters	Values
Pitch Circle Diameter of Runner (D_R)	155 mm
Rated RPM (N)	1500 rpm
Cross section area of shaft (A_s)	0.0008042 m^2
Polar moment of inertia of shaft about X axis (J_s)	5.1472×10-8 m^4
Area moment of inertia of shaft about Y or Z axis (I_s)	1.0294×10-7 m^4
Polar moment of inertia of disk about X axis (J_d)	0.5527×10-4 m^4
Area moment of inertia of disk about Y or Z axis (I_d)	0.11053×10-3 m^4
Length of shaft (L')	519 mm
Density of shaft material (ρ_s)	7860 kg/m^3
Young's Modulus of Elasticity of shaft (E)	202 GPa
Mass of rotating runner (M_d)	10.564 kg
Thickness of runner (h)	0.035 m
Mass polar moment of inertia of disk about x-x axis (J_{md})	0.0334 kgm^2
Mass moment of inertia of disk about y-y or z-z axis (I_{md})	0.0206 kgm^2
Nominal spin speed ($\Omega = 2\pi N/60$)	157.07 rad/s

3. Results

3.1 Shape functions and Equivalent Parameters

Solving Equation (22) for given system parameters, values of βL for the first three modes of vibration are obtained as shown in Table 2.

Table 2: Values of β L

First Mode	0.57680
Second Mode	1.12511
Third Mode	4.74416

Now, using Equation (23), the shape functions obtained are:

$$\phi_1 = cos(0.57680\frac{x}{L}) - cosh(0.57680\frac{x}{L}) - 1.27460(sin(0.57680\frac{x}{L}) - sinh(0.57680\frac{x}{L}))$$

$$\phi_2 = cos(1.12511\frac{x}{L}) - cosh(1.12511\frac{x}{L}) - 2.21274(sin(1.12511\frac{x}{L}) - sinh(1.12511\frac{x}{L}))$$

$$\phi_3 = cos(4.74416\frac{x}{L}) - cosh(4.74416\frac{x}{L}) - 0.98291(sin(4.74416\frac{x}{L}) - sinh(4.74416\frac{x}{L}))$$

Equations (15) to (18) are solved in Matrix Laboratory (MATLAB) using the above shape functions and equivalent parameters are obtained as shown in Table 3.

Table 3: Equivalent parameters

For first mode	For second mode	For third mode
ϕ_1	ϕ_2	ϕ_3
M_1= 0.67585 kg	M_2= 0.52879 kg	M_3= 0.66630 kg
C_1 = 1.35236Ω Ns/m	C_2=1.05868Ω Ns/m	C_3 = 1.43657Ω Ns/m
K_1 = 2247630.20231 - 0.67585Ω^2 N/m	K_2 = 40923956.49522 - 0.52878 N/m	K_3 = 5793877930.31206 - 0.66630Ω^2 N/m
F_1 = -0.25126 F(t)	F_2 = -0.21901 F(t)	F_3 = 0.02375 F(t)

3.2 Vibration Response

The equivalent parameters from Table 3 are used in equations (19) and solved using MATLAB to obtain the response of the cantilever shaft-disk system during startup and shutdown.

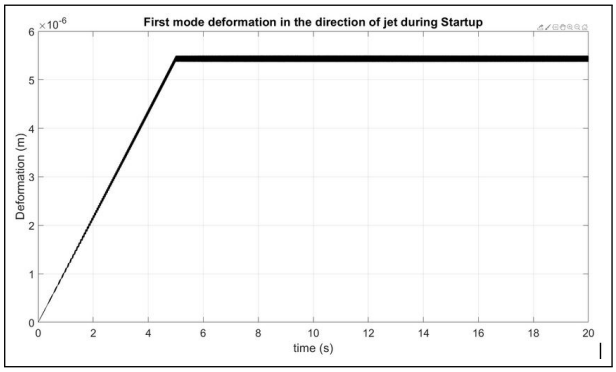

Figure 3: First mode response during startup

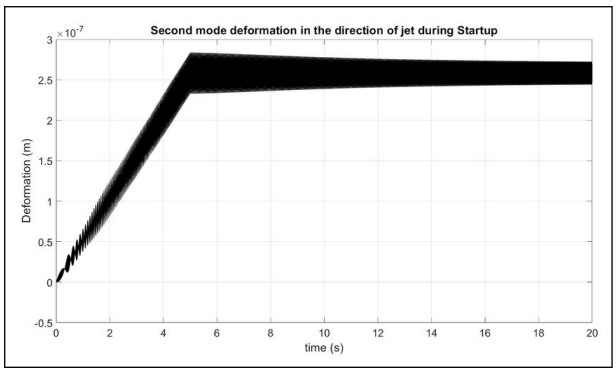

Figure 4: Second mode response during startup

Figures 3 and 4 show the response of a cantilever shaft-disk system during startup for the first two modes respectively. For the first mode, the maximum

deflection is around 5.5e-6m and for the second mode, it is around 0.3e-6m. The deflection in the third mode is negligibly low (order of 0.003e-6m) and thus not shown. The deflection is biased in direction opposite to the direction of water jet. A total deflection of around 5.8e-6m is expected during startup. It is also observed that the amplitude of vibration is minimal and the deflection stays constant at once the excitation force is steady i.e. no longer varying.

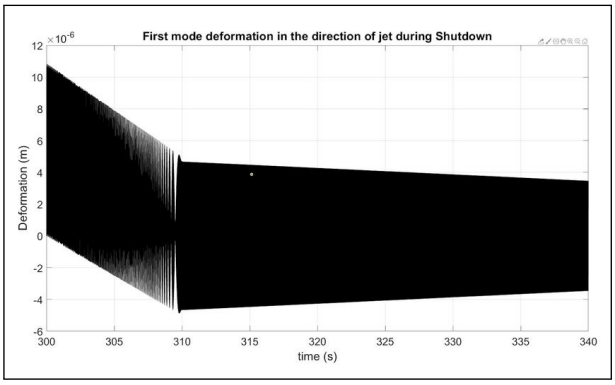

Figure 5: First mode response during shutdown

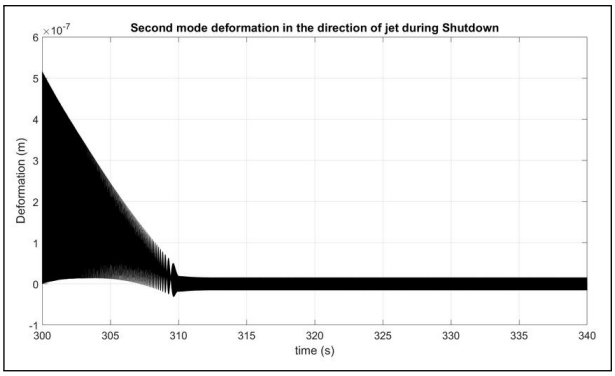

Figure 6: Second mode response during shutdown

Likewise, figures 5 and 6 show the response of a cantilever shaft-disk system during shutdown for the first two modes respectively. For the first mode, the maximum deflection is around 10.5e-6m and for the second mode, it is around 0.5e-6m only. Again, the deflection in the third mode is negligibly low (order of 0.02e-6m) and thus not shown. So a total deflection of around 11e-6m is expected during shutdown. Unlike startup condition, the amplitude of vibration is significant (around 5e-6m) during shutdown and once the water jet completely stops i.e. excitation force goes to zero, the amplitude starts decreasing with mean deformation of zero as expected for complete shutdown. The dark region after 310 seconds represents the steady state response of the system.

4. Conclusion

The characteristic equation for the cantilever Euler-Bernoulli beam with tip mass is derived and the shape functions for the first three modes of vibration are obtained analytically. The shape functions thus obtained are used to obtain equivalent mass, stiffness, damping and forcing functions for different modes of vibration. Finally, the governing second order differential equations are converted into a system of ordinary differential equations and solved with MATLAB. The maximum deflection that can be expected during startup and shutdown can be obtained by summing the deflections for the first two modes since the third mode has negligible deflection. Thus, for given system parameters, the expected maximum deflection during starting is around 5.8e-6m and during shutdown is around 11e-6m for the given choice of Pelton turbine. [5] did a similar study for a simply supported Pelton turbine and obtained similar order of deflection with peak shutdown deflection almost twice as that during startup. Results of this analysis show similar feature. This paper thus gives an insight on the transient response analysis of cantilever shaft-disk system.

Acknowledgments

The authors are thankful to the entire faculty of the Department of Mechanical and Aerospace Engineering, IOE, Pulchowk Campus, for their continuous technical support throughout the entire research process.

References

[1] HM Khanla, M Ghayour, and S Ziaei-Rad. Chaotic vibration analysis of rotating, flexible, continuous shaft-disk system with a rub-impact between the disk and the stator. 2011.

[2] Sanjeev Karki, Mahesh C. Luintel, and Laxman Poudel. Dynamic response of pelton turbine unit for forced vibration. 2017.

[3] Singiresu S. Rao. *Vibration of Continuous Systems*. John Wiley Sons, Inc., 2nd edition, 2019.

[4] David Mazurek E. Russel Johnston Ferdinand P. Beer, John T. DeWolf. *Mechanics of Materials*. McGraw-Hill Education, 6th edition, 2011.

[5] Bir B. Chaudhary. *Transient Response of Simply Supported Pelton Turbine During Starting and Shutdown*. 2022.